ELSEVIER

Journal of Structural Geology 27 (2005) 67–87

JOURNAL OF STRUCTURAL GEOLOGY

www.elsevier.com/locate/jsg

Morphology, intersections, and syn/late-diagenetic origin of vein networks in pelites of the Lodève Permian Basin, Southern France

Ghislain de Joussineau*, Loïc Bazalgette, Jean-Pierre Petit, Michel Lopez

Laboratoire de Dynamique de la Lithosphère (UMR 5573), c.c 060, Université Montpellier II, Place Eugène Bataillon, 34095 Montpellier cedex 5, France

Received 17 June 2003; received in revised form 22 January 2004; accepted 30 June 2004

Abstract

This paper presents the results of a field study aiming to describe and to interpret new types of relationships between vein sets. Three vein sets of the Lodève Permian Basin (Languedoc, Southern France) were studied. They consist of a family of N100E–N120E, widely opened sinuous veins with a composite infilling (sparite, calcite fibres, barite), hereafter called Sparitic Sinuous Veins, and of two orthogonal families of slim veins presenting a fibrous infilling of calcite, and oriented N10E–N20E and N90E–N100E, respectively. These two latter families are hereafter called N20 Fibrous Slim Veins and N90 Fibrous Slim Veins. The intersections between the three vein sets are shown to be original and more complex than those classically observed in the case of joint sets (abutting, crosscutting, …). The analysis of these intersections permitted a relative chronology of formation of the different vein sets to be established: the N20 Fibrous Slim Veins post-date the N90 Fibrous Slim Veins, which themselves post-date the Sparitic Sinuous Veins, the two former vein sets being shown to reopen contemporaneously.

Furthermore, the vein intersections were not as simple as expected. Indeed, the successive propagating cracks of one set could in certain cases crosscut the pre-existing veins of an earlier set, or could be stopped at contact with earlier veins in other cases. This implies a physical change in the interface between the pre-existing veins and the host rock (pelites) during the formation of the latest cracks.

Taking into account the well-known tectonic history of the Lodève basin, and the field observations (vein features, intersections, …), the origin of each vein set is discussed. We put forward that the Sparitic Sinuous Veins formed during the burial history of the basin: their morphological characteristics suggest that they appeared during the phase of active compaction of the basin, in response to the Permo-Triassic NS extension, and that their formation was assisted by fluid pressure. Second, we propose that the two orthogonal sets of Fibrous Slim Veins formed during the same extensional phase, their formation being favoured by the tectonic relaxation occurring at the beginning of the uplift of the basin at the end of the Permian. We attribute their particular characteristics (straight morphology of joints but systematic mineral infilling) to their origin in a medium already compacted but still incompletely lithified, and containing a large amount of fluids. We suggest that the fracturing history of the Lodève basin occurred in the time interval between the Late Permian (Thuringian) and the Middle Triassic (Anisian).

Finally, the observed evolution in the propagation path between the Sparitic Sinuous Veins and the N90 Fibrous Slim Veins is discussed, and bears out the idea that the rock material was not completely lithified when the vein sets formed.

Keywords: Vein intersections; Pelites; Lodève basin; Compaction; Burial and uplift; Thuringian; Anisian

1. Introduction

In spite of a hundred years' studies on joints (Pollard and Aydin, 1988) and veins (Durney and Ramsay, 1973; Hancock and Atiya, 1975; Ramsay, 1980; Cox, 1987; Urai et al., 1991) many fundamental aspects of mode I fracture morphology and genesis still have to be understood. A basic one is that of the morphological and mechanical transitions between joints (long and straight planar discontinuities showing opening displacements with no appreciable shear displacement) and veins (discontinuities often presenting en-échelon or sinuous geometries and significant opening but no shear displacement, filled by a cement derived from hydrothermal processes). These two fracture types are

* Corresponding author. Present address: Geological and Environmental Sciences Department, Stanford University, Stanford, CA934305, USA
E-mail address: dejoussi@stanford.edu (G. de Joussineau).

0191-8141/$ - see front matter © 2004 Elsevier Ltd. All rights reserved.
doi:10.1016/j.jsg.2004.06.016

usually considered as end members of mode I fractures (Bahat, 1991; Rives, 1992). However 'transitional' geometries (i.e. veins presenting morphological characteristics close to that of joints) are scarce. They deserve special attention in that they could help to determine the driving mechanisms leading to the various types. What do individual 'transitional' fractures and corresponding fracture network look like? Are they linked to given rock types or rheology? More generally, the mechanisms leading to mode I fracturing remain most often obscure and it would help to establish whether, in particular conditions, tensile stress of particular origins could generate particular types of mode I fractures, thus escaping the equifinality principle often evoked about jointing (Engelder, 1985, 1987; Laubach et al., 1998). Such an approach aiming to link a fracture network to its driving mechanisms needs a sharp and multiscale definition of 3D architecture of the fracture network including fractography and infilling within a well defined thermo-hydro-mechanical context.

In this paper we present such an attempt, based on the analysis of a fracture network developed in the Lodève Permian basin (Southern France), in a siliclastic environment (pelites and sandstones). The studied fractures consist of a nearly orthogonal network of mode I fractures. Some of them are clear veins, and others exhibit the rectilinear geometry and parallel distribution of joints but limited length, variable opening and calcite infilling, which may be seen as characters of veins. Thus they correspond to transitional mode I fractures, called 'Slim Veins' hereafter. The particular case of the Lodève basin enables us to address the following questions:

- What can we learn about the relative chronology and mechanisms of various mode I fracture sets when vein intersections are varied enough to push the analysis beyond the simple abutting/crosscutting relationships criteria (Hancock, 1985; Bahat, 1987; Rives et al., 1994)?
- What is the impact of high clay content both on morphology and driving mechanisms of mode I fractures, especially in the early steps of deformation?
- What are the characteristics of tectonic-related veins formed in incompletely lithified rocks, given that the aspects of soft-sediment deformation already described in the literature do not consist of organized fracture sets but include sedimentary structures [sediment flows (Jones and Omoto, 2000; Van Loon, 2002), loadcasts (Van Loon, 2002; Nogueira et al., 2003), slumps (Schwehr and Tauxe, 2003), laminations (Kawakami and Kawamura, 2002), …] and particular brittle structures [kink bands (Kimura et al., 1989), sigmoidal veins (Kimura et al., 1989; Brothers et al., 1996), faulting (Petit and Laville, 1987; Jones and Omoto, 2000; Van Loon, 2002), shear zones (Maltman, 1988; Kimura et al., 1989), …]?

At Lodève, the excellent outcropping conditions linked with quick erosion of the pelites in a Mediterranean climate permit the analysis of fractures sharply defined by their white calcite infilling within red pelites. This situation has triggered numerous field investigations concerning various aspects of the fracturing of the Lodève Permian basin such as geometry, organization, fractography, present-day fluid circulation, etc. (Santouil, 1980; Lopez, 1987; Rives, 1988; Pueo, 1993; Petit et al., 1994; Salti, 1995; Bruel, 1997; de Joussineau and Bazalgette, 1998; Jalabert, 1998; Bruel et al., 1999; Bazalgette, 2000). The widely studied regional context in terms of main tectonic events (listed in Saint Martin, 1992), sedimentology (Laversanne, 1976; Capus, 1979; Clément, 1986; Odin, 1986; Odin et al., 1986; Rolando et al., 1988; Lopez, 1992; Becq-Giraudon and Van Den Driessche, 1993) and geochemistry (Maury and Mervoyer, 1973; Bellon et al., 1974; Lancelot et al., 1984; Lévêque et al., 1988; Lancelot and Vella, 1989) help to discuss the tectono-mechanical origin of each fracture set and to propose a possible scenario in relation to the mechanical evolution at basin scale (Santouil, 1980; Horrenberger and Ruhland, 1981; Balmelle, 1989; Lopez, 1992).

Finally the studied fractured rocks, because of their clay content, raise the question of their top-seal properties in a half-graben basin, which can be seen as an excellent analogue of siliclastic oil and gas reservoirs.

2. Regional geologic setting

The studied areas are located in the 150-km^2 Lodève Permian basin, 60 km northwest from Montpellier, in southern France (Fig. 1a). The Lodève Permian basin forms a south dipping half graben covered unconformably by a thick horizontal Mesozoic cover (Fig. 1b). This cover is presently largely eroded, allowing the exposure of the basement and the Permian deposits. To the north, the Permian deposits onlap moderately folded non-metamorphic Cambrian carbonates and epimetamorphic Precambrian schists with vertical to moderate south dip. To the south and the east the EW-trending Les Aires Fault and the NE–SW-trending Cevennes Fault, respectively, limit the basin. These faults record both Upper Liassic extension and Pyrenean shortening, which preclude the observation of the original listric fault supposed to accommodate the southward tilting of the basement during the Permian (Saint Martin et al., 1990; Lopez, 1992).

2.1. Sedimentary architecture and stratigraphy of Permian deposits

The infilling of the basin is mainly composed of continental shales and pelite deposits that represent a present day thickness of more than 3000 m in the southern

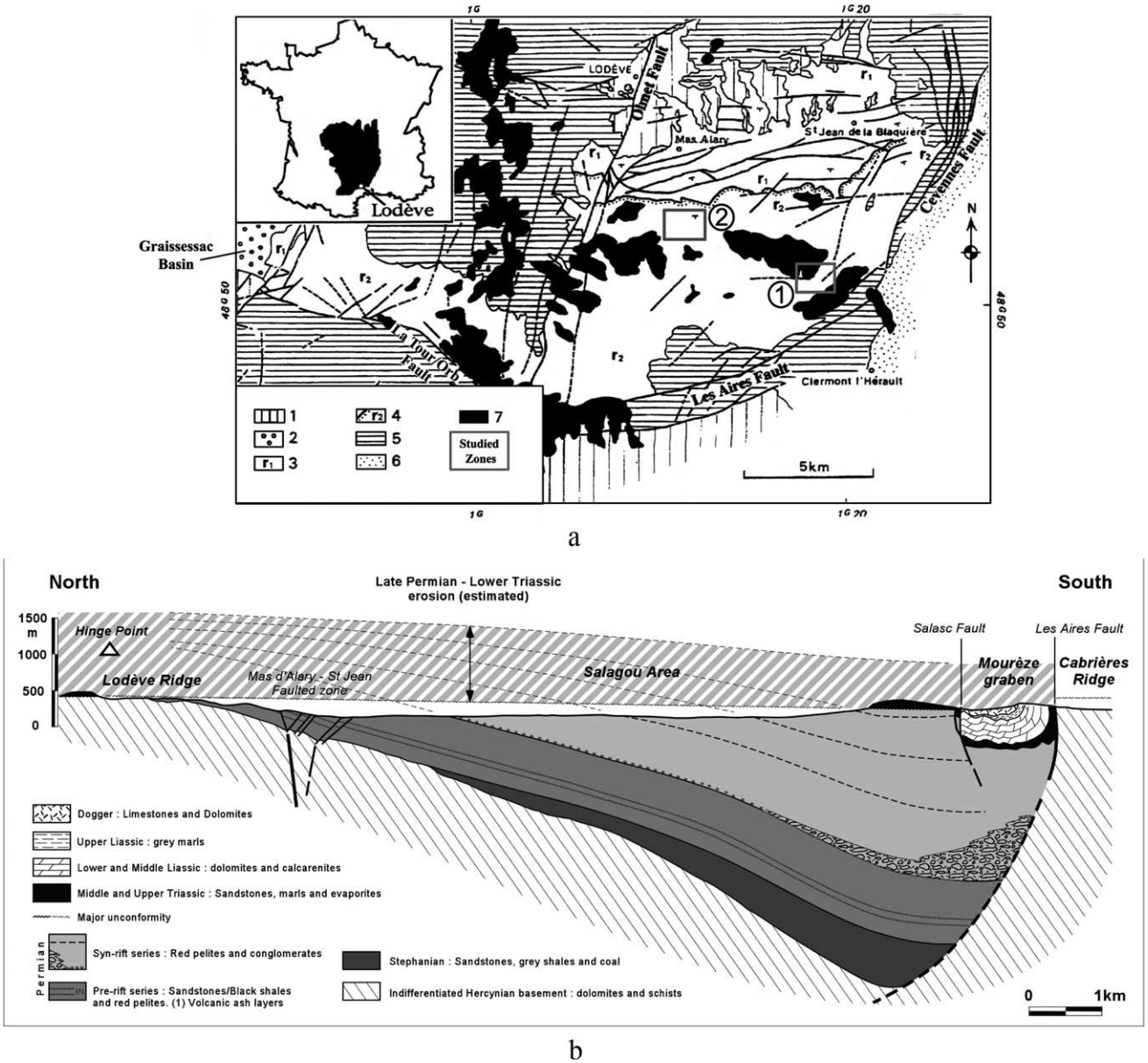

Fig. 1. (a) Structural map of the Lodève Permian basin (modified from Santouil, 1980). 1: Upper Precambrian and Lower Paleozoic basement rocks. 2: Stephanian formations of the Graissessac basin. 3: Autunian pile. 4: Saxono-Thuringian pelites. 5: Mesozoic carbonaceous cover. 6: Oligo-Miocene sandstones. 7: Plio-Quaternary alkali basalts. The location of the studied outcrops (1 and 2) is given. (b) Geological section of the Lodève Permian basin. The eroded thickness of sediments is estimated by Lopez (1992).

part of the basin near les Aires Fault. The Permian sequence records a major climate change from wet tropical to semi-arid in an extensive lacustrine to deltaic environment, clearly identified by an overall colour change of the sedimentary facies from grey to red (Laversanne, 1976). Odin (1986) divided the Permian sequence into five formations, which delineate the major changes in the depositional system. At the base of the series, the 250-m-thick Upper Autunian deposits display an overall drowning sequence. Alluvial fan conglomerates and breccias (0–100 m thick) locally entrenched in the Cambrian basement are extensively overlapped by fluvial to deltaic deposits (Usclas–St Privat Formation) which themselves evolve upward to anoxic deep lacustrine black shales and fine sandstones (Lower Tuilières–Loiras Formation). These organic matter-rich sediments were buried in the oil-window stage during the Thuringian and led to late oil and uranium migration (Laversanne, 1976; Capus, 1979). The Saxonian deposits are restricted to the 200-m-thick Upper Tuilière–Loiras Formation, which shows similar facies interposed with red pelites/fine sandstones (Saint Martin et al., 1990) indicating seasonal tropical wet and dry alternation in a global shallowing upward cycle. Finally, this tendency continues during the Thuringian where more than

2000 m of pelite-dominated sediments were deposited in a shallow to sub-emersive environment from floodplain (Viala Formation), alluvial fan and delta (Rabejac Formation), to sub-emersive playa lake (Salagou Formation). Transport directions measured on channel axis and current bedforms both indicate that the detrital material comes from the western part of the basin, where the pelite facies of the Salagou Formation passes abruptly to stacked debris-flow deposits (La Tour-sur-Orb facies). The Permian deposits are unconformably covered by Middle Anisian sandstones and conglomerates, which extend beyond the basin (Fig. 1b).

2.2. Tectonic history of the Lodève Permian Basin

The Lodève basin was related to a late orogenic extension in response to the gravity collapse of the Hercynian chain (Van Den Driessche, 1992). During the Late Carboniferous, the uplift of the gneiss dome of the axial zone of the Montagne Noire occurred in response to the isostatic readjustment of the thick Hercynian crust. This phenomenon led to the opening of an EW elongated basin on the northern part of the present day basin by inversion of previous thrusts as extensional shear zones (Echtler and Malavieille, 1990). This initial basin extended during the Lower to Middle Permian indicating a whole NS extensional regime with a relative homogeneous subsidence evidenced by a constant sediment thickness throughout the basin (Lopez, 1992). During the lower Thuringian (Rabejac Formation), the activation of the listric fault on the southern border of the basin led to the progressive southward tilting of the basement and previous Permian deposits. During the time interval between the Upper Thuringian and the Middle Anisian, the basin and its borders were submitted to an extensive subaerial erosion with deep palaeosoil development that caused the removal of about 1500 m of the uppermost sediments (Lopez, 1992). This deconfinement of the basin may have played an important role in deep overpressurized fluid relaxation and joint development. Neither the extensional faulting in response to the opening of the Tethian ocean during the Jurassic nor the Oligocene N110 extension linked to the opening of the western Mediterranean domain are evidenced in the basin. Only the Paleocene–Eocene Pyrenean NS compression is recorded in the basin by small inversions and limited strike-slip reactivations (Bruel et al., 1999). Finally, during the Plio-Quaternary, a poorly understood event resulted in alkali-basalt emplacement along a NS trend. The present day slight NS compression measured throughout the basin is possibly inherited from this period.

Because the thick pelite infilling of the basin is very homogeneous and isolated from post-Permian tectonics, fault and joint development could easily be related to the well-constrained syn-tectonic activity of the basin.

2.3. Studied areas

Most of our observations are located in the eastern part of the basin, in particular close to the Salagou dam (Area 1, Fig. 1a). The pile consists of Thuringian sequences formed of metre-thick red pelites (composed of 70% clay and 30% silt; Odin et al., 1986) alternating with thin beds of sandstone whose thickness is generally less than 10 cm. Most of these sandstone beds exhibit mud cracks. Layers dip 5°S to 10°S, due to the Permian extensional phase. A second area was studied in the northwestern part of the basin (Area 2, Fig. 1a), near the Mas Delon hamlet. This area is situated stratigraphically below the area of the Salagou dam. In terms of sedimentary facies, the most important difference between the two studied areas concerns the thickness of the sandstone beds interposed with the red pelites, which is often more than 30 cm in the Mas Delon area, and less than 10 cm in the Salagou dam area.

3. Description of fracture sets

Three vein sets that do not pass into the Triassic cover and characterised by different orientations and morphologies have been observed in the Permian stratigraphic section (Fig. 2).

3.1. Sparitic Sinuous Veins

The most obvious set shown in Fig. 2 (set 1 = Sinous Sparitic Veins = SSV) consists of sinuous veins with variable apertures from one to several centimetres along a given vein. This set is organized in several-metres-long segmented systems. They show frequent hooking and branching geometries. The orientation of the veins varies from N100E to N120E, and their dip is essentially perpendicular to bedding. Their infilling mainly consists of sparite crystals, but frequently contains host rock chips and vugs of calcite/barite (Fig. 3a). Fibrous calcite is sometimes observed on the wall of the veins (Fig. 3a). Numerous outcrops next to the Salagou dam show that these veins are folded vertically, thus evidencing a vertical shortening after the calcite infilling (Fig. 3a and b). This shortening of the veins is clearly posterior to their propagation and does not result from growth under constraints. Indeed, at contact with the shortened Sinuous Sparitic Veins, the pelites and some tiny fibrous veins exhibit a similar shortening (Fig. 3b).

The Sinuous Sparitic Veins present diverging lineations representing an uncommon style of coarse plumose structures, which evidence dominant vertical or horizontal mode I propagations according to the cases. Several observations suggest that the veins initiated at the sandstone beds. Little round structures are irregularly distributed on the surfaces of the veins (Fig. 3c). Cross-sections of these asperities (Fig. 3d) systematically show inclusions of pelite

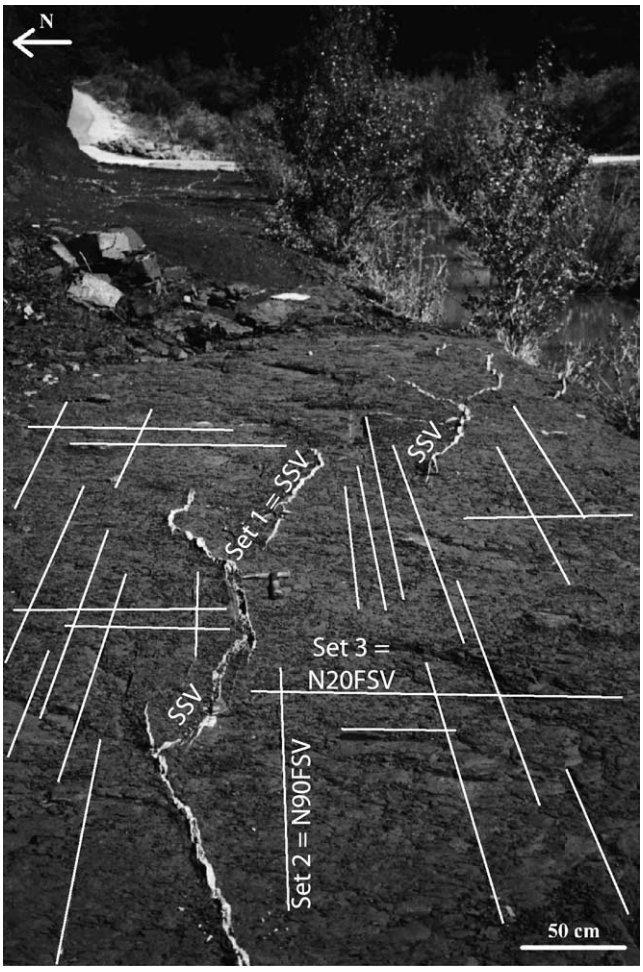

Fig. 2. Fracture pattern in the Salagou dam outcrop (two sets are underlined): Set 1: N90 Sparitic Sinuous Veins organized in 3D systems (SSV). Set 2: N90 Fibrous Slim Veins (N90FSV). Set 3: N20 Fibrous Slim Veins (N20FSV). The same abbreviations are used for the different vein sets in the following figures.

in the calcite infilling. This enables us to interpret these structures as a consequence of a difference of mechanical behaviour of sparite and pelite during the vertical shortening: the deformation of sparite in response to the vertical shortening pushed aside on the pelites, softer than the sparite (the irregular morphology of the veins being easily imprinted in the pelites), leading to the formation of the observed structures. Observations of the veins on horizontal surfaces and cliffs enable a 3D reconstruction to be realized (Fig. 3e), showing that the connectivity between the different parts of the same system strongly evolves vertically. The presence of hooks and en-échelon cracks (commonly thought to form under slow propagation) and of hackles and branching fractures (implying dynamic fracturing) along the Sinuous Sparitic Veins suggest that their propagation occurred at various velocities, which had been suggested by Auzias et al. (1993).

Finally, the Sinuous Sparitic Veins exhibit small dip-slip displacements (less than 10 cm) marked by the offset of the thin sandstone horizons.

In the northern parts of the Lodève basin (Mas Delon area), these Sparitic Sinuous Veins tend to be straighter (but not linear) with fewer hooking and branching tendencies but a systematic presence of fibrous calcite in their infilling.

3.2. Fibrous Slim Veins

The second type of fractures forming an orthogonal set (sets 2 and 3, Fig. 2) may represent transitional fractures between joints and veins: indeed, due to their linear geometry, their small aspect ratio, and their distribution into strictly parallel sets, they are close to joints; but due to the systematic presence of a calcite infilling and their relatively limited trace length, they are close to veins. We propose to call these fractures *Slim Veins*.

3.2.1. N90 Fibrous Slim Veins

A first set of slim veins (Fig. 2: set 2 = N90 Fibrous Slim Veins = N90FSV) is N90E–N100E-trending, i.e. nearly parallel to the Sparitic Sinuous Veins. It consists of several-metres-long parallel veins. The spacing between these veins is irregular, ranging from a few tens of centimetres to a few metres. Their infilling is clearly fibrous, but with calcite crystals not as elongated as in the N20 Fibrous Slim Veins (see below). Crack-seal is frequent and evidenced by the presence of small parallel pelite inclusions within the calcite infilling (Ramsay, 1980). Several stages of opening are evidenced by successive generations of fibres (t_1, t_2 and t_3 in Fig. 4a). Maximum thickness is irregular, ranging from less than 1 mm to more than 1 cm. In front view plumose geometries show that these veins are pure mode I fractures (Bahat, 1991) and that they systematically initiated at thin beds of sandstone (Fig. 4b). Their dip is perpendicular to bedding.

3.2.2. N20 Fibrous Slim Veins

The second set of slim veins (Fig. 2: set 3 = N20 Fibrous Slim Veins = N20FSV) is N10E–N20E-trending, i.e. perpendicular to the mean direction of N90 Fibrous Slim Veins and Sparitic Sinuous Veins. Its macroscopic features are similar to those of the N90 Fibrous Slim Veins (straight parallel veins, Fig. 4c). The spacing between the veins is irregular, ranging from 10 cm to several metres in the same area. Their infilling consists of thin antitaxial or syntaxial fibrous calcite (Ramsay and Huber, 1983), some fibres being coloured by the clayey impurities (Fig. 4d). As observed in N90 Fibrous Slim Veins, several stages of opening can be evidenced (t_1 and t_2 in Fig. 4d), the total thickness of the calcite infilling ranging from less than 0.2 mm to 5 mm. The dip of these veins is roughly perpendicular to bedding. Conversely to the Sparitic Sinuous Veins, the N20/N90 Fibrous Slim Veins are not folded vertically.

Fig. 5 represents the main geometrical relationships between the three vein sets. First, the global density of Fibrous Slim Veins is important (with respect to the thickness of the beds) but varies laterally: when the set of

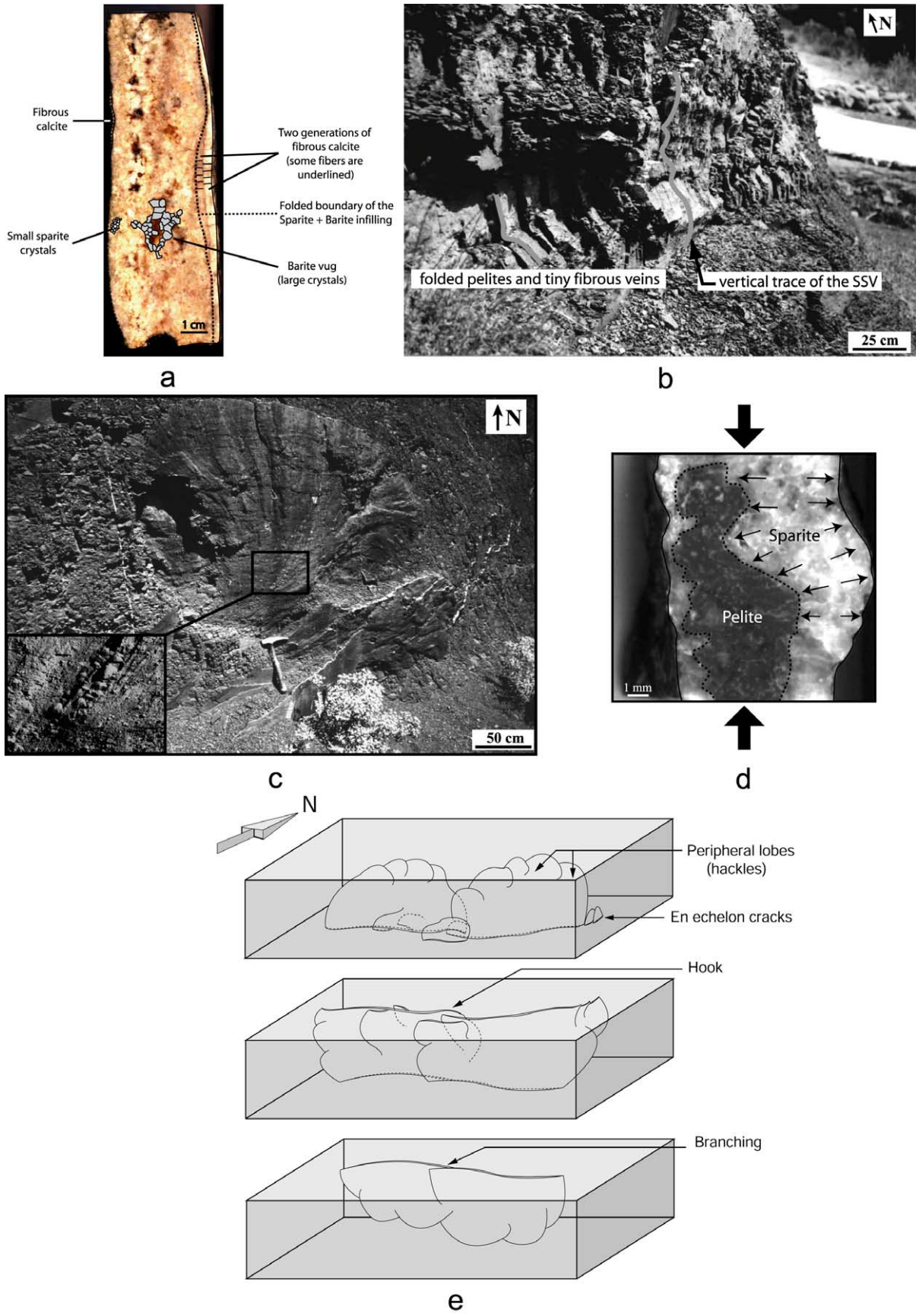

Fig. 3. (a) Typical infilling of a Sparitic Sinuous Vein in the Mas Delon area, containing small crystals of sparite, barite vugs and fibrous calcite. (b) Section view of a Sparitic Sinuous Vein evidencing its vertical folding (Salagou dam outcrop). At contact with the vein, both the pelites and some tiny fibrous veins exhibit similar folding. (c) Front view of a Sparitic Sinuous Vein, showing fractographic features and small round structures (Salagou dam outcrop). (d) Section across a round structure (black arrows indicate the vertical shortening): pelite is systematically included in the vein infilling. (e) 3D reconstitution of a Sparitic Sinuous Vein system of the Salagou dam area, deduced from cliff observations and subhorizontal surfaces.

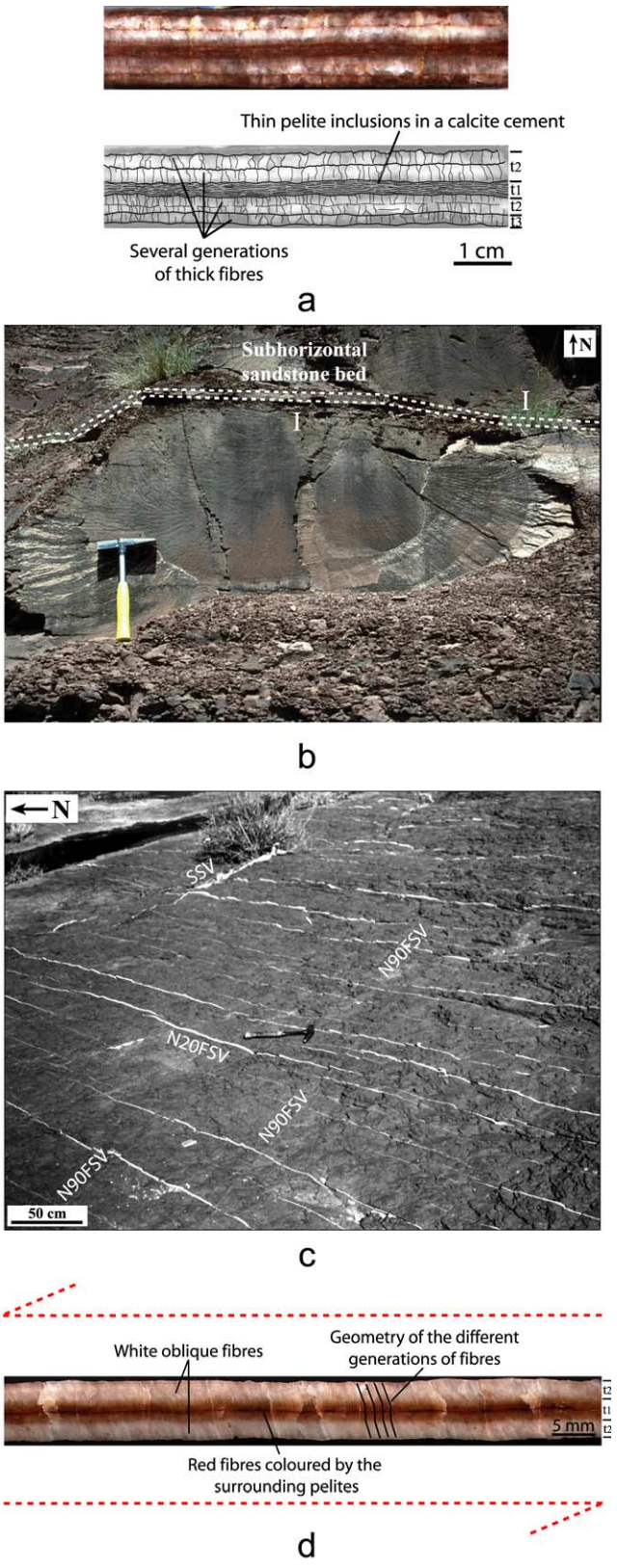

Fig. 4. (a) Interpreted photograph of a N90 Fibrous Slim Vein showing several stages of opening. The first generation of calcite (t_1) contains small pelite inclusions, which are markers of crack-seal. (b) Cliff view of two N90 Fibrous Slim Veins initiating at a sandstone bed. The initiation of the fractures, deduced from the fractographic features on their surface, is marked by an I on the photograph. (c) Photograph showing particularly dense and opened N20 Fibrous Slim Veins near the dam of the Salagou lake. (d) Interpreted photograph of a N20 Fibrous Slim Vein showing several stages of opening, including a stage of strike-slip (t_2).

N20 Fibrous Slim Veins is dense, the orthogonal set (N90 Fibrous Slim Veins) is less dense with less opened veins, and reciprocally. It is shown that both Sparitic Sinuous Veins and Fibrous Slim Veins initiate at sandstone beds, which acted as tensile stress concentrators. Typically, the Fibrous Slim Veins are vertically limited by successive sandstone beds, which can act both as initiation (source) or impeding (barrier) discontinuities during the fracture propagation (Petit et al., 1994). However, several cases showing Fibrous Slim Veins unable to crosscut the pelite layers totally have been found.

Finally, a geochemical study using the rubidium/strontium method indicates that the $^{87}Sr/^{86}Sr$ signatures of the calcite infillings of the two sets of Fibrous Slim Veins are identical, and comparable with that of the calcite cement of the host rock (Jalabert, 1998).

4. Description and chronological interpretation of relationships between vein sets

We carefully examined all the observed types of intersections between the vein sets, which permitted us to establish a possible scenario and timing for the joint and vein development through the Permian pile. The photographs and corresponding interpretative sketches presented below illustrate the most common relationships between the three studied vein sets.

4.1. Sparitic Sinuous Veins VS N90 Fibrous Slim Veins

Because of their similar orientations, these two sets rarely intersect. Fig. 6a and b illustrates the most common type of relationships between the two sets: a N90 Fibrous Slim Vein is deflected along a Sparitic Sinuous Vein and becomes tangent to it. Fibres remain perpendicular to the walls even at contact with the Sparitic Sinuous Vein. This situation where the Fibrous Slim Vein trajectory is deviated by a Sparitic Sinuous Vein demonstrates that the N90 Fibrous Slim Veins propagated after the Sparitic Sinuous Veins, as presented in the Fig. 6c scenario.

4.2. Sparitic Sinuous Veins VS N20 Fibrous Slim Veins

Four types of interactions are observed between these two sets, presented from the most common to the least frequent At the contact with Sparitic Sinuous Veins:

(a) Some N20 Fibrous Slim Veins tend to be divided into several very thin veins, some of them being stopped at contact with a Sparitic Sinuous Vein, whereas others

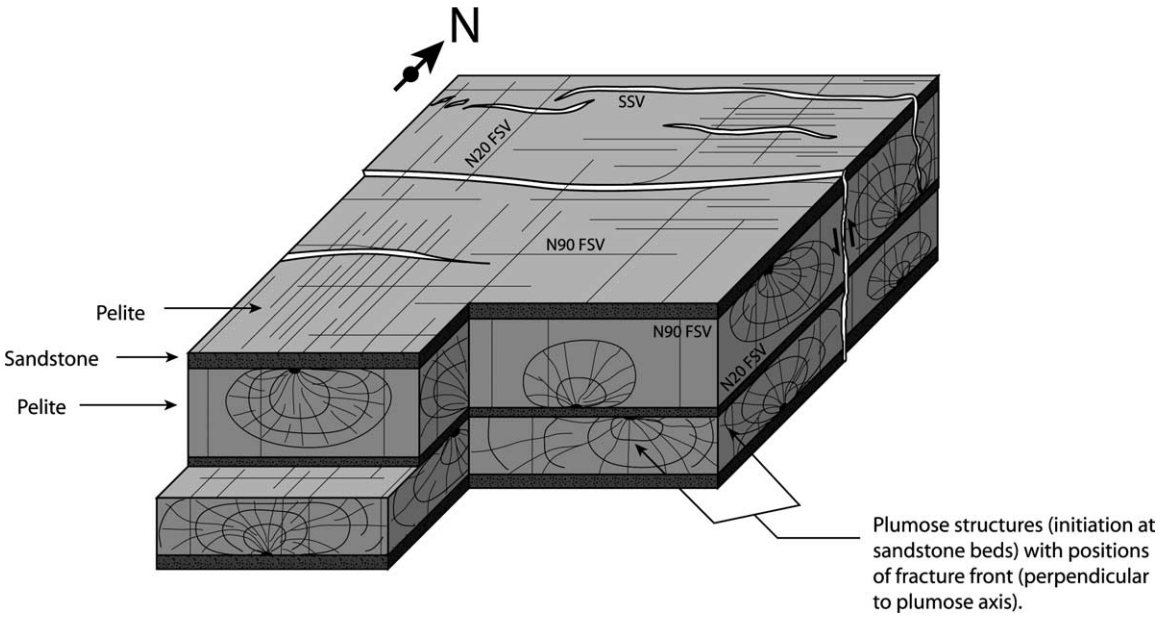

Fig. 5. 3D drawing presenting the relations between the vein sets and the sedimentary layers in the Salagou dam area. Note the irregular density of the two sets of Fibrous Slim Veins.

totally crosscut the infilling of the Sparitic Sinuous Vein (Fig. 7a and b). This relationship evidences that the Sparitic Sinuous Veins pre-date the N20 Fibrous Slim Veins (Fig. 7c). This situation is frequent.

(b) The aperture of some N20 Fibrous Slim Veins suddenly decreases to zero at contact with a Sparitic Sinuous Vein (Fig. 8a and b). This implies the pre-existence of Sparitic Sinuous Veins, whose infilling impeded the propagation of N20 Fibrous Slim Veins but did not prevent further aperture (Fig. 8c). This situation is frequent.

(c) Some N20 Fibrous Slim Veins make an angle to become parallel to Sparitic Sinuous Veins and localize at their surface (Fig. 9a and b). This infrequent geometry is

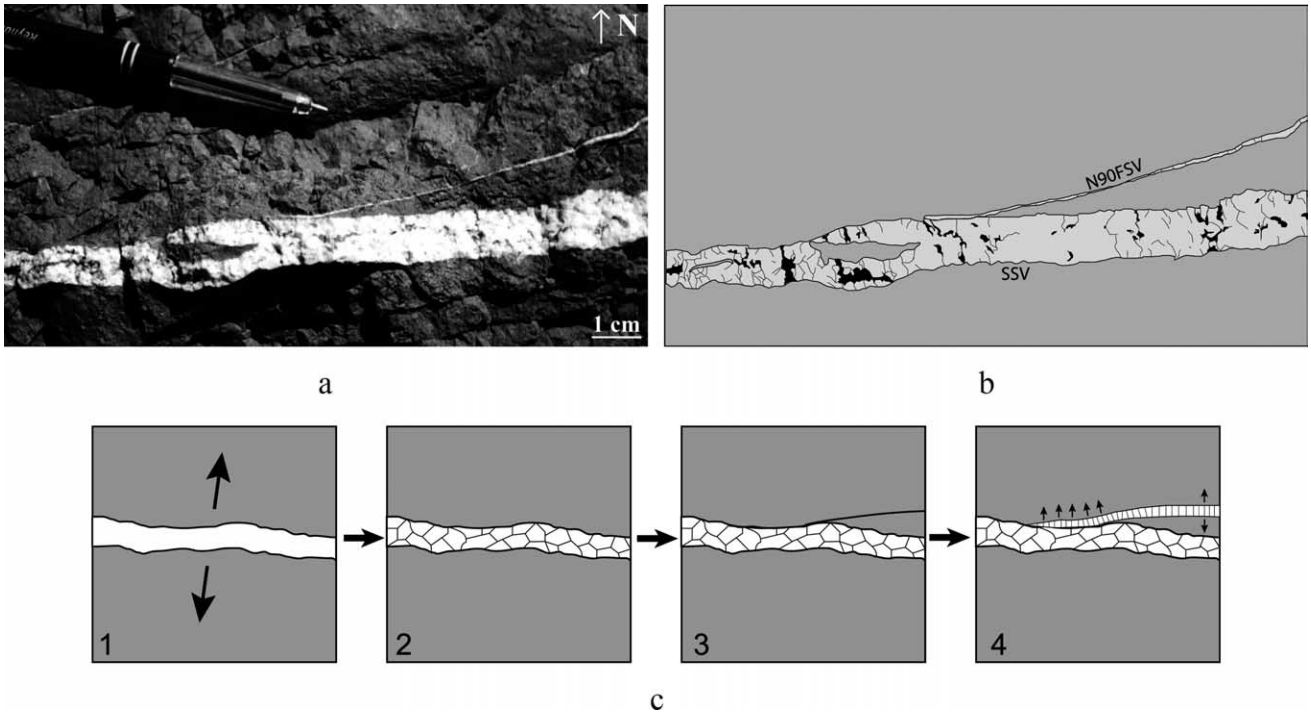

Fig. 6. (a) Photograph of a N90 Fibrous Slim Vein deviated at contact with a Sparitic Sinuous Vein. (b) Drawing corresponding to the photograph. (c) Proposed scenario for the development of the observed intersection.

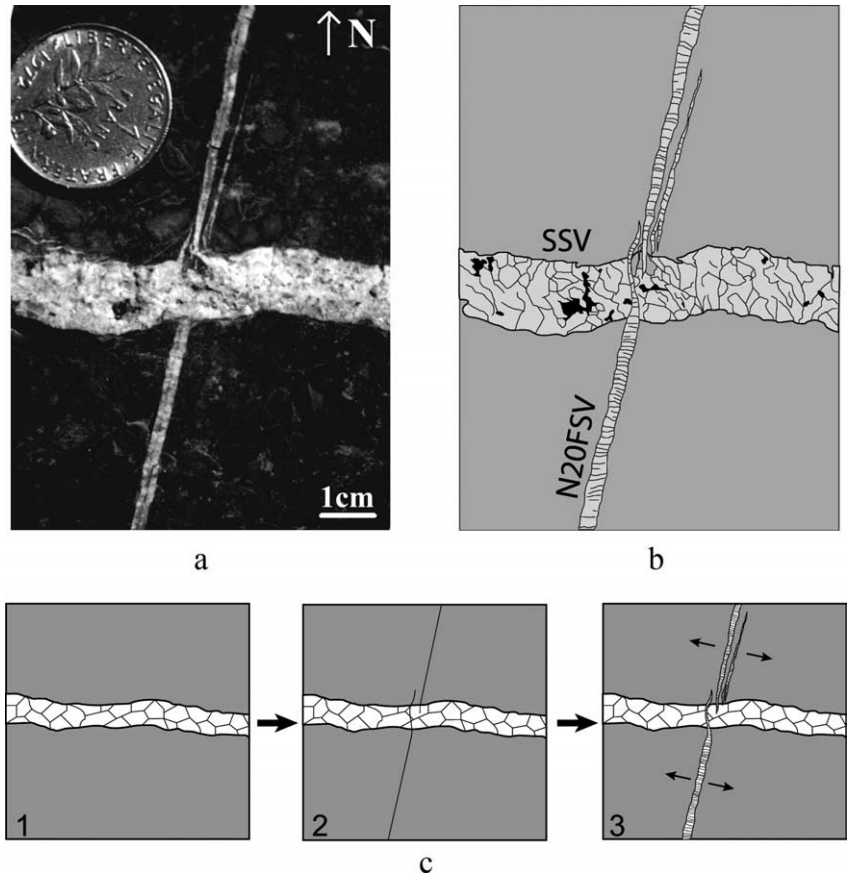

Fig. 7. (a) Photograph of two N20 Fibrous Slim Veins getting thinner at contact with a Sparitic Sinuous Vein, and partially crosscutting its infilling. (b) Drawing corresponding to the photograph. (c) Proposed scenario for the development of the observed intersection.

somewhat similar to that described in Fig. 6 and implies again the pre-existence of the Sparitic Sinuous Veins (Fig. 9c). A biaxial aperture is evidenced.

(d) Some N20 Fibrous Slim Veins crosscut Sparitic Sinuous Veins (Fig. 10a and b). This implies that the N20 Fibrous Slim Veins propagated and broke the existing infilling of the Sparitic Sinuous Veins (Fig. 10c). This situation is very rare.

All these interactions show that the Sparitic Sinuous Veins formed before the N20 Fibrous Slim Veins, but also show that the Sparitic Sinuous Veins could either prevent the propagation of N20 Fibrous Slim Veins or not.

4.3. N90 Fibrous Slim Veins vs N20 Fibrous Slim Veins

These two sets show a great variety of situations.

We present the five most demonstrative ones, from the most frequent to the least frequent case:

(a) Offsets of N90 Fibrous Slim Veins by N20 Fibrous Slim Veins are observed (Fig. 11a and b): this implies that the N20 Fibrous Slim Veins propagated across a pre-existent N90 Fibrous Slim Vein. Afterwards, two possible scenarios are proposed (Fig. 11c): (1) the N20 crack was affected by a right-lateral strike-slip movement, and was mineralised during a subsequent opening step; (2) the N20 crack was mineralised before the offset. The fact that the fibres within the N20 Fibrous Slim Vein are always perpendicular to its walls indicates that the strike-slip movement was not contemporaneous to an opening stage (Ramsay and Huber, 1983). This situation is frequent.

(b) As illustrated by Fig. 12a and b (and with the same geometry as in Fig. 11), clear crosscutting intersections are observed, which imply that N20 Fibrous Slim Veins post-dated N90 Fibrous Slim Veins (Fig. 12c). These situations are common.

(c) A more complex intersection is illustrated by Fig. 13a and b. Its interpretation (Fig. 13c) is that after the propagation of the N20 crack through the pre-existent N90 Fibrous Slim Vein, a left-lateral strike-slip movement along its walls displaced the N90 Fibrous Slim Vein. The opening of the N20 Fibrous Slim Vein occurred in a later stage, in a manner that implies a transform interfacial slip between the N90 Fibrous Slim Vein and the host rock. Two separate apertures were necessary to form two adjacent generations of fibres (overlap) between the two parts of the N90 Fibrous Slim Vein. This situation is rare.

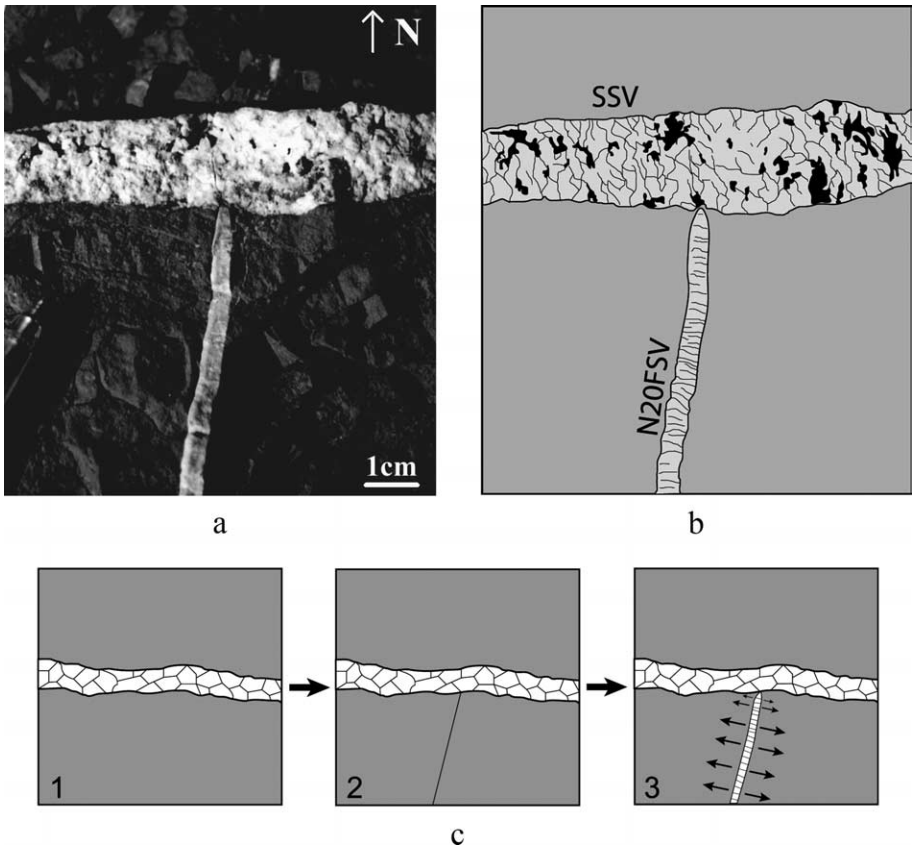

Fig. 8. (a) Photograph of a N20 Fibrous Slim Vein stopped at contact with a Sparitic Sinuous Vein. (b) Drawing corresponding to the photograph. (c) Proposed scenario for the development of the observed intersection.

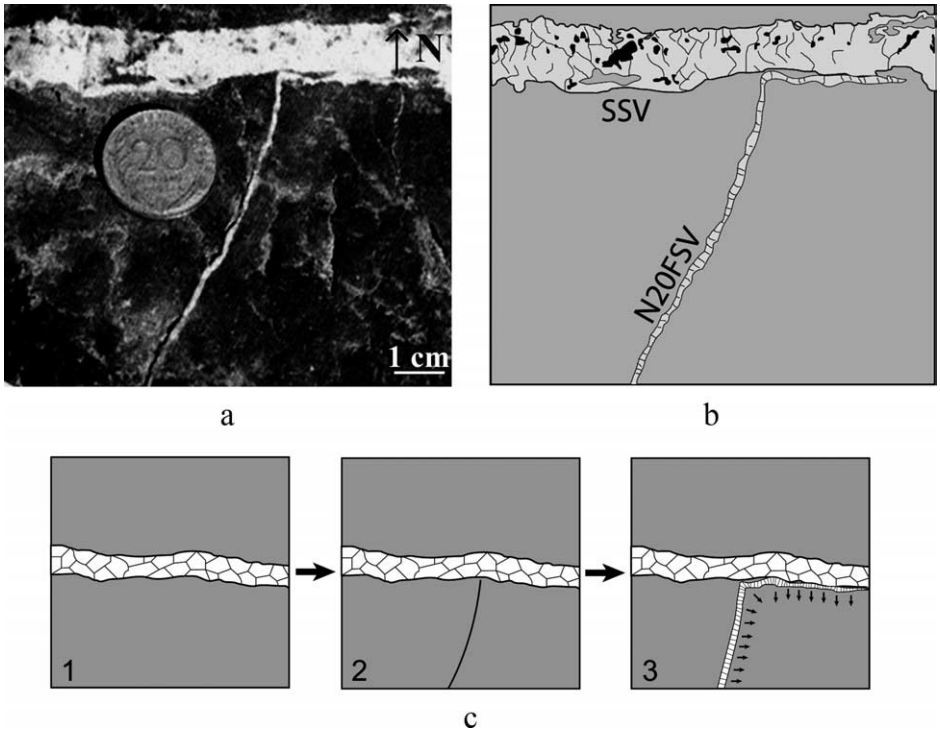

Fig. 9. (a) Photograph of a N20 Fibrous Slim Vein deviated at contact with a Sparitic Sinuous Vein. (b) Drawing corresponding to the photograph. (c) Proposed scenario for the development of the observed intersection.

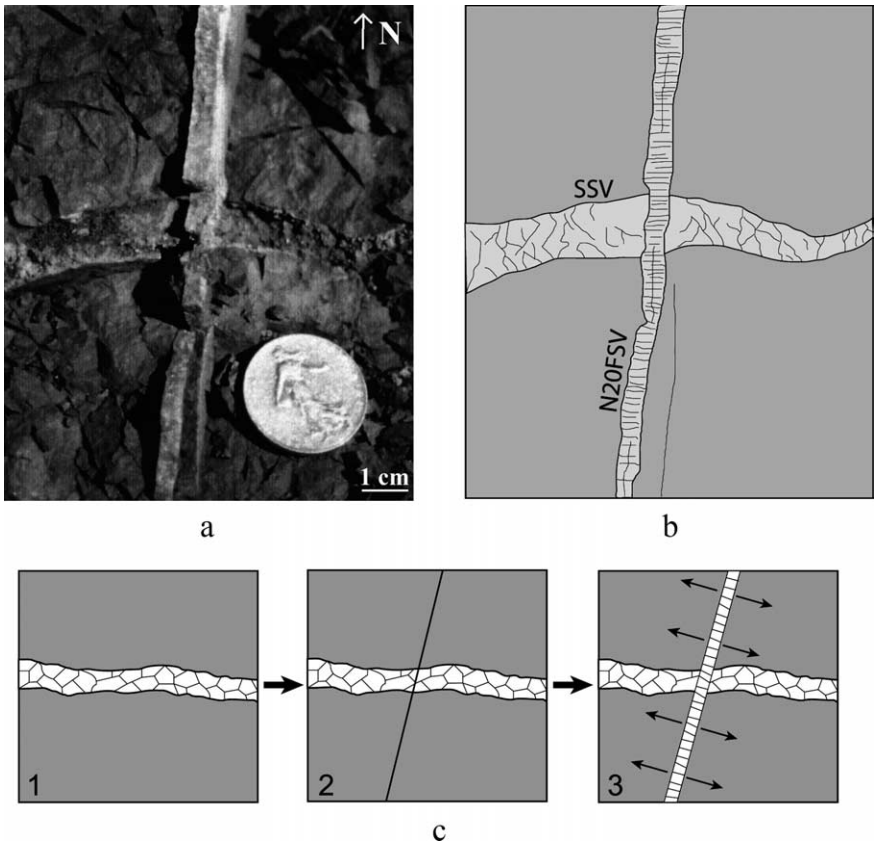

Fig. 10. (a) Photograph of a N20 Fibrous Slim Vein crosscutting a Sparitic Sinuous Vein. (b) Drawing corresponding to the photograph. (c) Proposed scenario for the development of the observed intersection.

(d) Finally, one single example was found with a hook geometry of two N20 Fibrous Slim Veins at contact with a N90 Fibrous Slim Vein (Fig. 14a and b). It clearly suggests that the N20 Fibrous Slim Veins post-dated the N90 Fibrous Slim Vein (Fig. 14c).

In summary the N20 Fibrous Slim Veins post-date the N90 Fibrous Slim Veins. However, this chronology is not totally strict: Fig. 15 shows the detailed analysis of an intersection where two N20 Fibrous Slim Veins are divided into many thin veins next to the contact with a N90 Fibrous Slim Vein, showing its influence on the propagation of N20 Fibrous Slim Veins. However, the thin veins crosscut only the lower part of the N90 Fibrous Slim Vein with crack-seal, but not the upper part, which implies a second stage of opening of the N90 Fibrous Slim Vein after the propagation of the N20 Fibrous Slim Veins (the N20 Fibrous Slim Veins are later than the N90 Fibrous Slim Veins, but may be contemporaneous with the late stages of N90 opening).

From all the presented observations, we established the following chronology between the different fracture sets: the N20 Fibrous Slim Veins post-date the N90 Fibrous Slim Veins, which themselves post-date the Sparitic Sinuous Veins.

5. Mechanical interpretation of the vein intersections.

5.1. Evidences for a mechanical evolution in the vein intersections

Two different types of contacts may be distinguished from the previous paragraph: the first type includes all the intersections where the propagating crack crosscuts the pre-existing vein (‘crosscutting’ intersection types: Figs. 7 and 10–15), and the second type includes the intersections where the propagating crack was not able to crosscut the pre-existing vein (‘deflecting’ intersections and interruptions: Figs. 6, 8 and 9). An interesting point in understanding the mechanisms of these two intersection types is found in Pollard and Aydin (1988), Helgeson and Aydin (1991), and Cooke and Underwood (2001). These authors suggest that the ability or inability of a crack to propagate across an interface (in our case, the interface is the contact between the rock material and the surfaces of the pre-existing veins) mainly depends on the strength of this interface. If the interface is weak (i.e. is open, or is closed but can slip), the crack will not propagate across it, and will tend to stop, or to be deflected along this interface. Conversely, if the interface is strong (i.e. is closed and

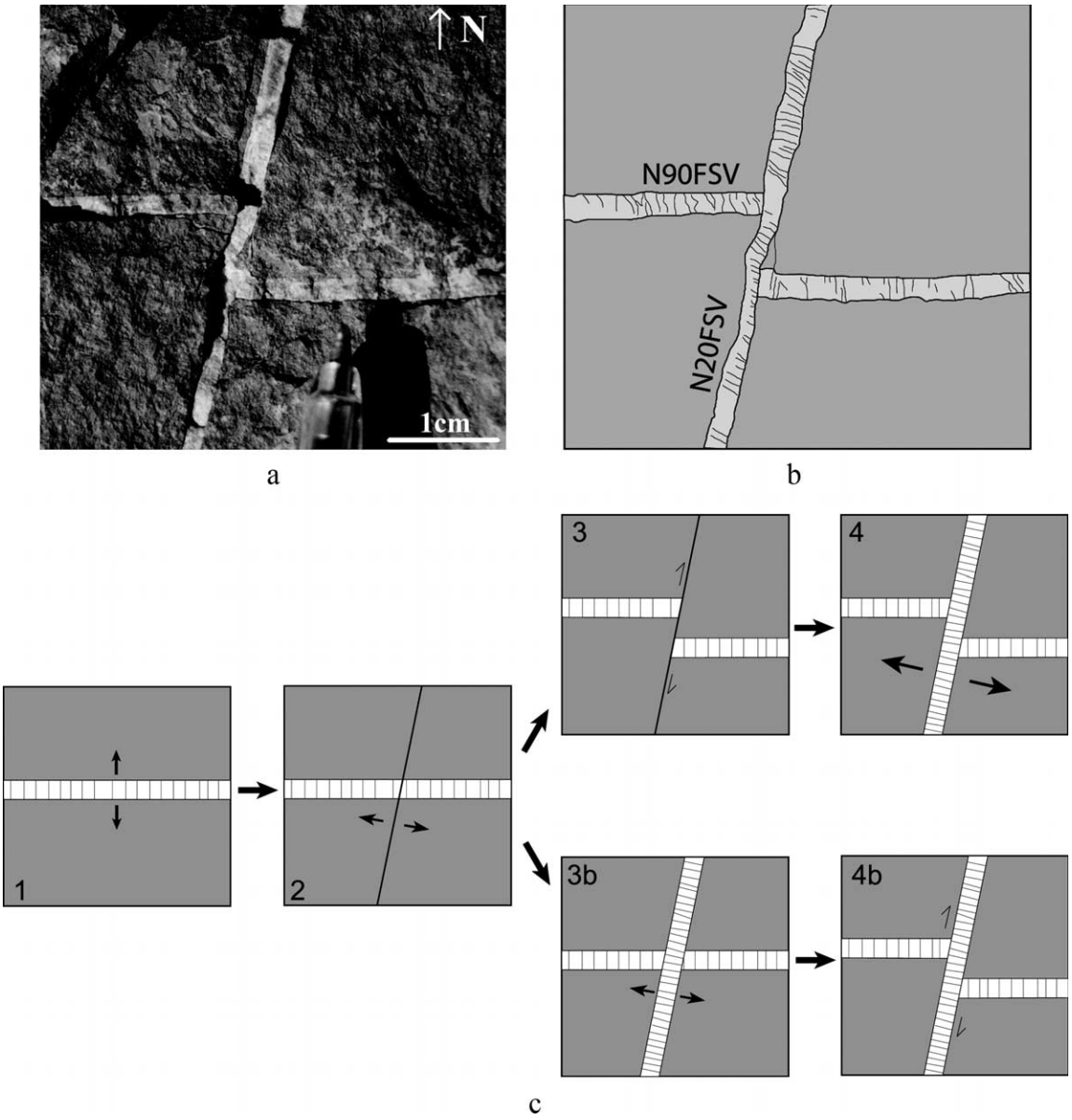

Fig. 11. (a) Photograph of a N20 Fibrous Slim Vein crosscutting and displacing a N90 Fibrous Slim Vein. (b) Drawing corresponding to the photograph. (c) Proposed scenario (two different possibilities) for the development of the observed intersection.

cannot slip because of high friction, cohesion, …), the crack will be able to propagate across it.

In the case of the relationships between the Fibrous Slim Veins (N20 Fibrous Slim Veins and N90 Fibrous Slim Veins) and the Sparitic Sinuous Veins, we observed that the main tendency for the appearing crack was not to propagate across the Sparitic Sinuous Veins, although rare observations of N20 Fibrous Slim Veins crosscutting Sparitic Sinuous Veins exist. As a consequence, the interfaces between the surfaces of the Sparitic Sinuous Veins and the pelites were probably weak when the Fibrous Slim Veins propagated, even if scarce evidences for significantly strong interfaces between the Sparitic Sinuous Veins walls and the pelites can be found. Conversely, in the case of the relationships between the N90 Fibrous Slim Veins and the N20 Fibrous Slim Veins, we only noticed crosscutting intersections, and the interfaces between the surfaces of the N90 Fibrous Slim Veins and the pelites probably acted as relatively strong interfaces during the propagation of the N20 Fibrous Slim Veins.

There seems to be a progressive evolution in the mechanisms of the vein intersections in the Lodève basin: indeed we previously established that the first veins to form were the Sparitic Sinuous Veins (1), followed by the N90 Fibrous Slim Veins (2), and finally by the N20 Fibrous Slim Veins (3), and the interfaces were mainly weak when the earliest Fibrous Slim Veins formed (see the relationships between the Sparitic Sinuous Veins and the N90 Fibrous

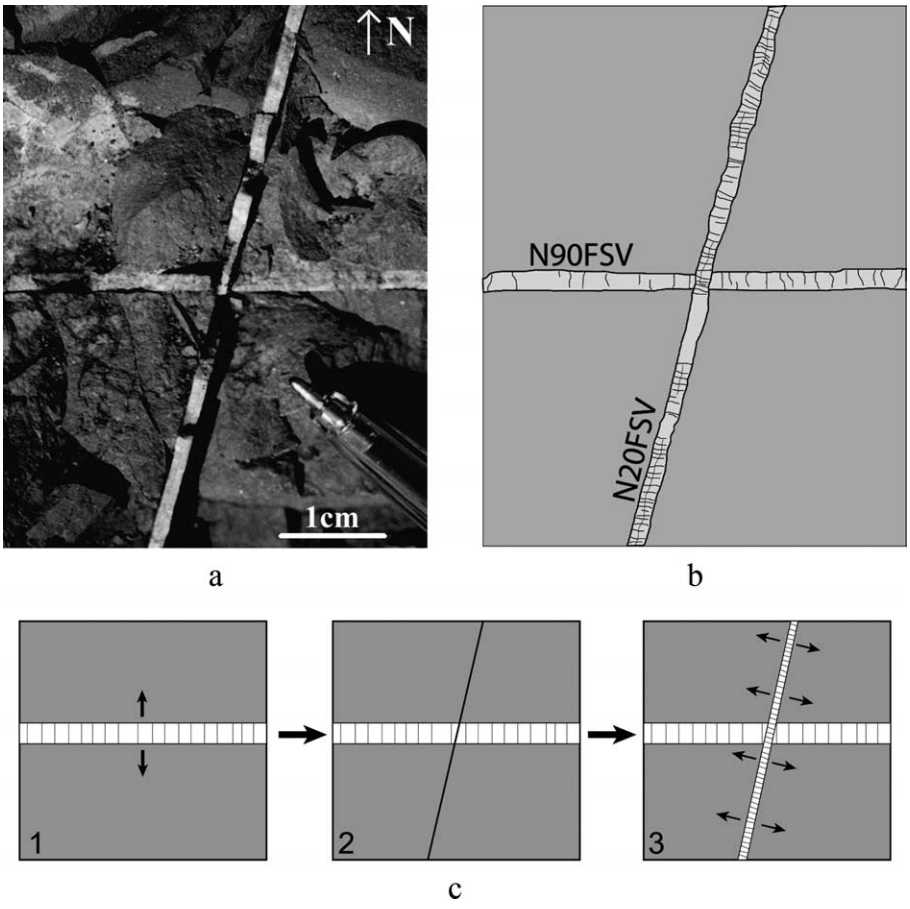

Fig. 12. (a) Photograph of a N20 Fibrous Slim Vein crosscutting a N90 Fibrous Slim Vein. (b) Drawing corresponding to the photograph. (c) Proposed scenario for the development of the observed intersection.

Slim Veins), and were mainly strong/cohesive when the latest Fibrous Slim Veins formed (relationships between the N90 Fibrous Slim Veins and the N20 Fibrous Slim Veins). This mechanical evolution is illustrated by the relationships between the Sparitic Sinuous Veins and the N20 Fibrous Slim Veins: from Fig. 9 (deflection of a N20 Fibrous Slim Vein along a Sparitic Sinuous Vein) to Fig. 10 (a N20 Fibrous Slim Vein crosscuts a Sparitic Sinuous Vein), an evolution towards increasingly strong interfaces between the surfaces of the Sparitic Sinuous Veins and the rock material is evidenced, with intermediary stages (Fig. 8: a N20 Fibrous Slim Vein stops at contact with a Sparitic Sinuous Vein; Fig. 7: two N20 Fibrous Slim Veins get thinner in contact with a Sparitic Sinuous Vein and partially/totally break its infilling).

5.2. Proposed mechanism

To explain the observed evolution in the mechanical state of the interfaces between the pre-existing veins and the pelites, a mechanism implying a physical change in the host rock (pelites) is needed, because the stiffness/cohesion of the Sparitic Sinuous Veins calcite infilling is not expected to have evolved during the propagation of the Fibrous Slim Veins (no evidence of dissolution–recristallization was found in the Sparitic Sinuous Veins infilling).

The Sparitic Sinuous Veins are the only veins that were folded vertically, implying their early origin during a sedimentary interval not completely compacted nor lithified. Conversely, the Fibrous Slim Veins, because of their planar and rectilinear shape, propagated in an already compacted medium: in these conditions, the compaction of the basin does not seem to be the likely mechanism provoking a change in the physical state of the medium during the propagation of the Fibrous Slim Veins.

We then propose that a late-diagenetic stage of lithification of the pelites, occurring during the propagation of the Fibrous Slim Veins, may account for increasingly strong/-cohesive interfaces between the calcite infilling of the Sparitic Sinuous Veins and the host rock. Indeed, the progressive diagenesis of the pelites, resulting in a decrease in the mechanical contrast between the Sparitic Sinuous Vein infilling and the host rock, may explain why cracks of a same family could in certain cases stop at contact with pre-existing veins or could in other cases crosscut their infilling. Fig. 16 summarizes the different types of relationships existing between the N20 Fibrous Slim Veins and the Sparitic Sinuous Veins, and proposes to link such a variety

of vein intersections with an increasing lithification/stiffness of the pelites (i.e. with a decreasing mechanical contrast between the calcite infilling of the pre-existing veins and the pelites).

Several facts/observations support the hypothesis of a still active diagenesis of the pelites during the propagation of the Fibrous Slim Veins. Indeed, the pelites contain a variable but sometimes important number of calcite vacuoles. These vacuoles (mineralised gas bubbles resulting from pedologic evolution of a soil in sub-emersive conditions) are filled by a transparent calcite cement (Fig. 15), and this calcite of local origin (depositional calcite) has shown to be comparable with the calcite infilling of the Fibrous Slim Veins in terms of $^{87}Sr/^{86}Sr$ signature. This strongly suggests that the calcite infilling of the Fibrous Slim Veins derives from the stock of in-situ fluid trapped in the pores of the pelites during the burial of the basin, implying that the host rock was still incompletely dewatered/lithified when the Fibrous Slim Veins propagated. Furthermore, the N90 Fibrous Slim Veins frequently exhibit crack-seal features (Figs. 4a and 15), and the crack-seal phenomenon implies consecutive episodes of excess in-fluid pressure, which may be caused by a progressive cementation of the medium (Laubach, 1988). We propose that, in the Lodève basin, the last stages of lithification of the pelites resulted in the progressive cementation of the medium and in the precipitation of a calcite infilling in the propagating/existing fractures (Fibrous Slim Veins), leading to increasingly strong/cohesive interfaces between the pre-existing Sparitic Sinuous Veins and the pelites.

6. Possible origin of the studied veins

We examine here the possible origin of the three vein sets, i.e. the possible mechanisms that led to the formation of each studied vein set.

6.1. Sparitic Sinuous Veins

From the vein intersections described above, we established that the first existing veins of the Lodève basin were the Sparitic Sinuous Veins. The fact that they were submitted to the compaction of the basin (they are vertically folded) indicates that they formed very early in still soft sediments. We propose that they were associated with the Permo-Triassic NS extension of the basin, and that they formed during the subsidence of the basin (i.e. during the burial of the sediments). Indeed, many N90E–N110E faults of the basement were reactivated as normal faults in the Lodève basin area during this tectonic phase (Santouil, 1980; Bruel, 1997). The soft deposits of the basin, situated above these normal faults, were tilted and deformed partly because of their activity. The orientation of the Sparitic Sinuous Veins (N100E–N120E) is compatible with a formation during the Permo-Triassic stage of NS extension, and furthermore, these veins exhibit small vertical offsets indicating that they acted as small normal faults. We propose that the driving mechanisms leading to the formation of the Sparitic Sinuous Veins are a combination of both the Permo-Triassic extensional regime and fluid pressure. Indeed, their morphology is close to that of experimental fractures obtained when injecting a plaster solution in gelatin in a controlled stress field (Bazalgette, 2000). The origin of the fluids resulting in the future Sparitic Sinuous Veins infilling may be found in the sandstone beds (the veins initiated at sandstone beds, and fluids are known to migrate easily in the horizontal direction within the permeable sandstone beds; Magara, 1976), in the water-rich pelites, or in both the sandstones and pelites. This scenario combining the role of the stress regime and the injection of pressurized fluids in the propagating fractures accounts for both the complex morphology of Sparitic Sinuous Veins and their early origin at shallow depth in incompletely compacted pelites. Even if the development of fractures at shallow depth during the burial of sediments is not very common, this phenomenon has been evidenced by Bahat (1989), who described fracture sets formed at very shallow depth (100 m) during the burial history of Eocene chalks in Israel.

We note that the Sparitic Sinuous Veins do not correspond to the two end member mode I fracture types forming during burial following Engelder (1985): they are neither hydraulic mode I fractures [the pelites of the Lodève basin were buried at a maximum depth of 3 km (Lopez, 1992) and the natural hydraulic fracturing usually requires burial depths of 5–6 km; Magara, 1975, 1981], nor tectonic mode I fractures: they probably formed in a very early stage of burial at relatively shallow depth, and not at significant depth in response to abnormal pore pressure induced by a horizontal tectonic compression.

6.2. Fibrous Slim Veins

The Fibrous Slim Veins formed in a material that was completely compacted and incompletely lithified. This indicates that they may have formed at the end of the burial (no more active compaction), during the Permo-Triassic history of the Lodève basin (incomplete dewatering of the pelites). Furthermore, the N20 Fibrous Slim Veins post-date the N90 Fibrous Slim Veins, but late stages of N20/N90 opening indicate that the two sets were reopened contemporaneously. We propose that the two sets of Fibrous Slim Veins formed during the Late Thuringian–Scythian uplift of the basin, caused by the important erosion of the Permian deposits (Lopez, 1992). The orientation of the N90 Fibrous Slim Veins is compatible with the NS Permo-Triassic extensional regime, which may explain why they formed before the N20 Fibrous Slim Veins, in the early stage of relaxation of the basin (most favourable direction). The local fluids may have assisted the formation of the N90 Fibrous Slim Veins because crack-seal, indicating

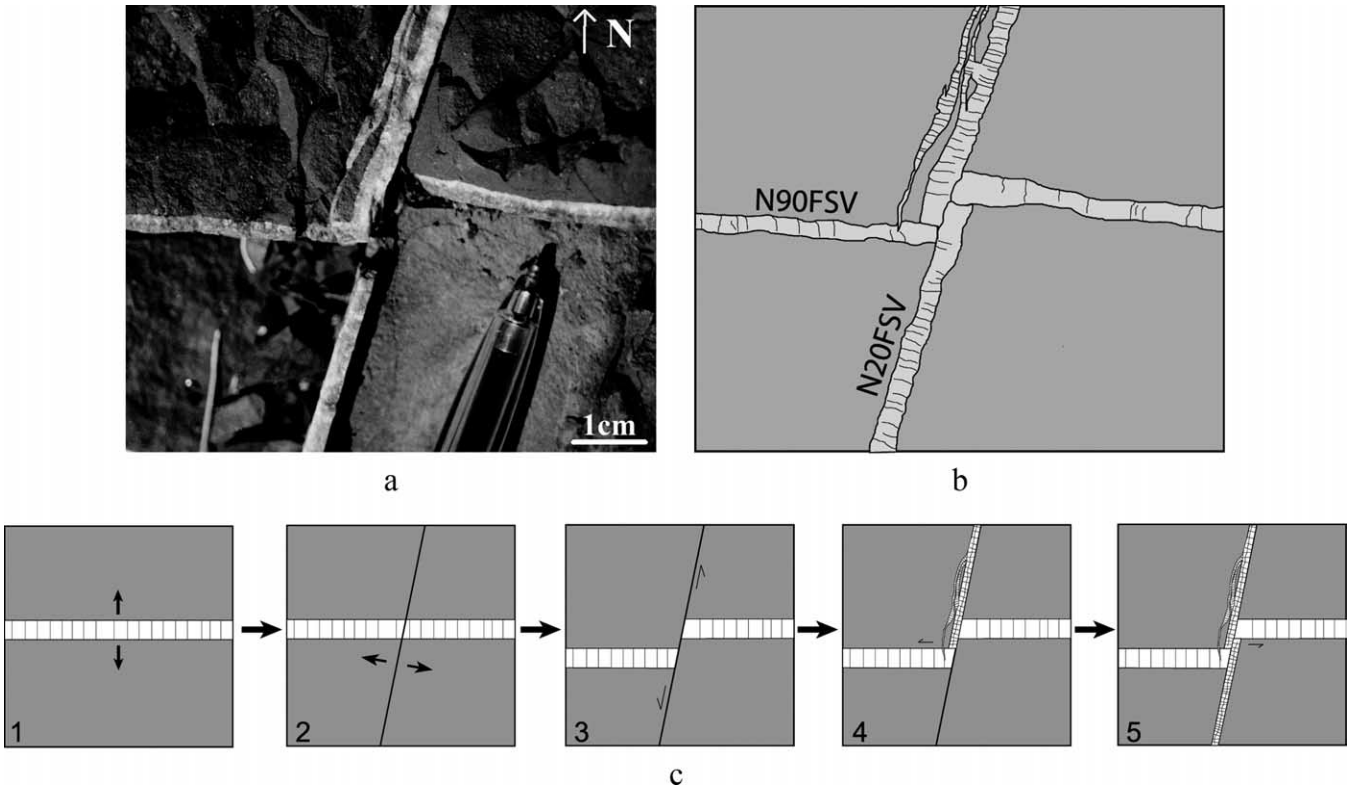

Fig. 13. (a) Photograph of a N20 Fibrous Slim Vein crosscutting and displacing a N90 Fibrous Slim Vein. (b) Drawing corresponding to the photograph. (c) Proposed scenario for the development of the observed intersection.

successive excess in-fluid pressure, is recorded in their infilling. Reversals between the two close horizontal principal stresses $S_H = \sigma_2$ and $S_h = \sigma_3$ (in an extensional regime, the maximum principal stress σ_1 is expected to be vertical; Rives et al., 1994) may account for the formation of N20 Fibrous Slim Veins and the successive reopening stages of the two sets. Indeed, the formation of the N90 Fibrous Slim Veins perpendicular to σ_3 releasing the tension in this direction, the consequent stress drop would be sufficient to reverse the directions of σ_2 and σ_3, leading to the formation of a new set of fractures perpendicular to the N90 Fibrous Slim Veins, the N20 Fibrous Slim Veins (Simon et al., 1988). A similar mechanism of reversal between σ_2 and σ_3 is proposed by Gauthier and Angelier (1986) for the formation of orthogonal sets of mode I fractures in the extensional regime of the Suez Rift.

Finally, the small strike-slip movements observed along some N20 Fibrous Slim Veins (Figs. 4d, 11 and 13) may be very early (evidences of grain reductions and alignments of pelite fragments have been found in N20 Fibrous Slim Veins infilling), or may be slight manifestations of the Pyrenean phase of NS compression occurring during the Palaeocene–Eocene. Indeed, this major tectonic phase reactivated some faults in the Salagou dam area, and affected the Cévennes Fault (Bruel, 1997).

The Permian extensional regime, the stress relaxation caused by the uplift of the basin, and the relaxation of the pressurized fluids trapped in the pores of the pelites all played a role in the formation of the Fibrous Slim Veins. The progressive opening of the veins, associated with the progressive drainage of the medium, account for their fibrous infilling.

A possible scenario for the formation of the three studied vein sets of the Lodève basin is shown in Fig. 17 (we know neither the time interval during which each vein set formed, nor the time interval existing between the end of the Sparitic Sinuous Vein formation and the beginning of the Fibrous Slim Vein formation): the whole fracturing history of the basin lies between the late Permian (Thuringian) and the middle Triassic (Anisian).

The successive steps of fracturing leading to the formation of the three studied vein sets are presented in Fig. 18. The Sparitic Sinuous Veins formed in soft sediments and were submitted to the strongest phase of compaction of the basin (Fig. 18b and c), then the N90 Fibrous Slim Veins propagated in still soft sediments (Fig. 18d), and the N20 Fibrous Slim Veins propagated in increasingly stiff sediments (Fig. 18e–g).

7. Propagation paths of the studied vein sets

We examine here the origin of the change in the fracture propagation paths occurring during the fracturing history of

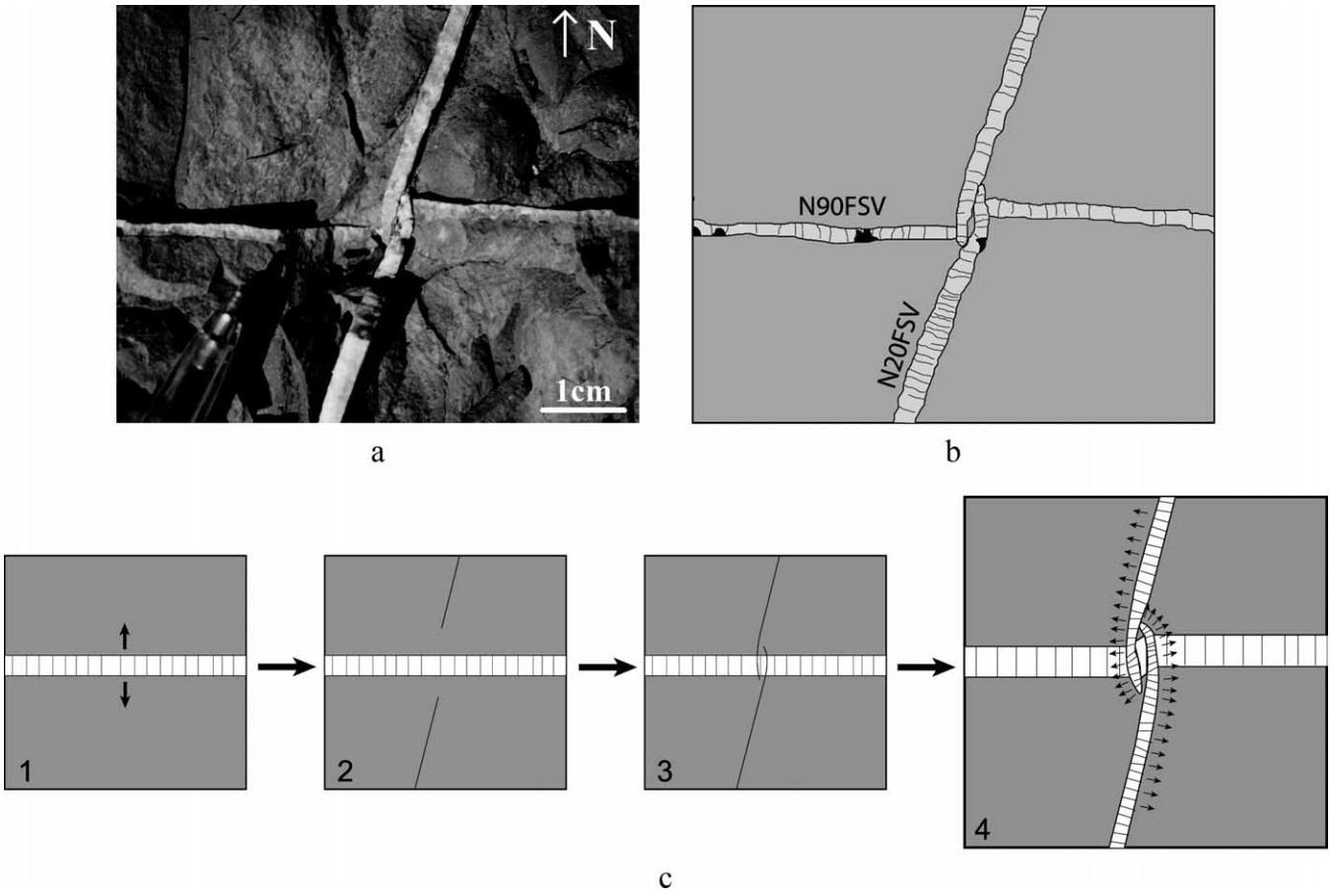

Fig. 14. (a) Photograph of two N20 Fibrous Slim Veins converging to form a hook through a N90 Fibrous Slim Vein. (b) Drawing corresponding to the photograph. (c) Proposed scenario for the development of the observed intersection.

the Lodève basin: the older vein set corresponds to opened sinuous veins organized in 3D systems (Sparitic Sinuous Veins), and the two younger vein sets correspond to straight veins (Fibrous Slim Veins). We propose that they formed in an early stage of the basin history, i.e. during the Permo-Triassic NS extension. In these conditions, what can explain the difference in the propagation path between the Sparitic Sinuous Veins (sinuous) and the N90 Fibrous Slim Veins (straight), given that their orientations are similar?

The existing studies devoted to the geometry of fracture propagation paths linked the ability of a crack to propagate in a straight direction to a strong differential stress in the medium (Olson and Pollard, 1989), and also proposed that the tendency of a crack to propagate in a straight or curved manner directly depends on the value of the stress ratio $R = [(\sqrt{\pi a})(S_H - S_h)]/K$ (Renshaw and Pollard, 1994), where a is half of the length of the considered fracture, $(S_H - S_h)$ is the differential stress existing in the medium and K is the stress intensity factor at the tips of the considered fracture (critical or sub-critical stress intensity factor). The greater that R is (i.e. the greater the differential stress $(S_H - S_h)$ or the smaller K), the straighter the propagation of the fracture.

We think that the stress ratio theory is not applicable in the Lodève basin, for two reasons. First, the stress ratio theory concerns fracture growth geometries in linear elastic materials, and the mechanical behaviour of the Lodève pelites was probably significantly different from a pure linear elastic behaviour at least during the Sparitic Sinuous Veins propagation (material incompletely compacted/dewatered). The rheology of such incompletely lithified materials is poorly known, but they are not expected to behave as pure elastic materials, partly because of their incomplete cohesion. Second, the variations in the differential stress $(S_H - S_h)$ occurring in the Lodève basin during the propagation of the Sparitic Sinuous Veins and the N90 Fibrous Slim Veins are not well known, but this differential stress was probably small when the slim veins propagated because these two orthogonal sets formed and reopened contemporaneously: the stress ratio theory fails in the case of the Fibrous Slim Veins because it predicts sinuous propagation paths when the differential stress is small, but the slim veins are straight.

We propose that the observed difference in the propagation paths between the Sparitic Sinuous Veins and the N90 Fibrous Slim Veins lies in the mechanical evolution

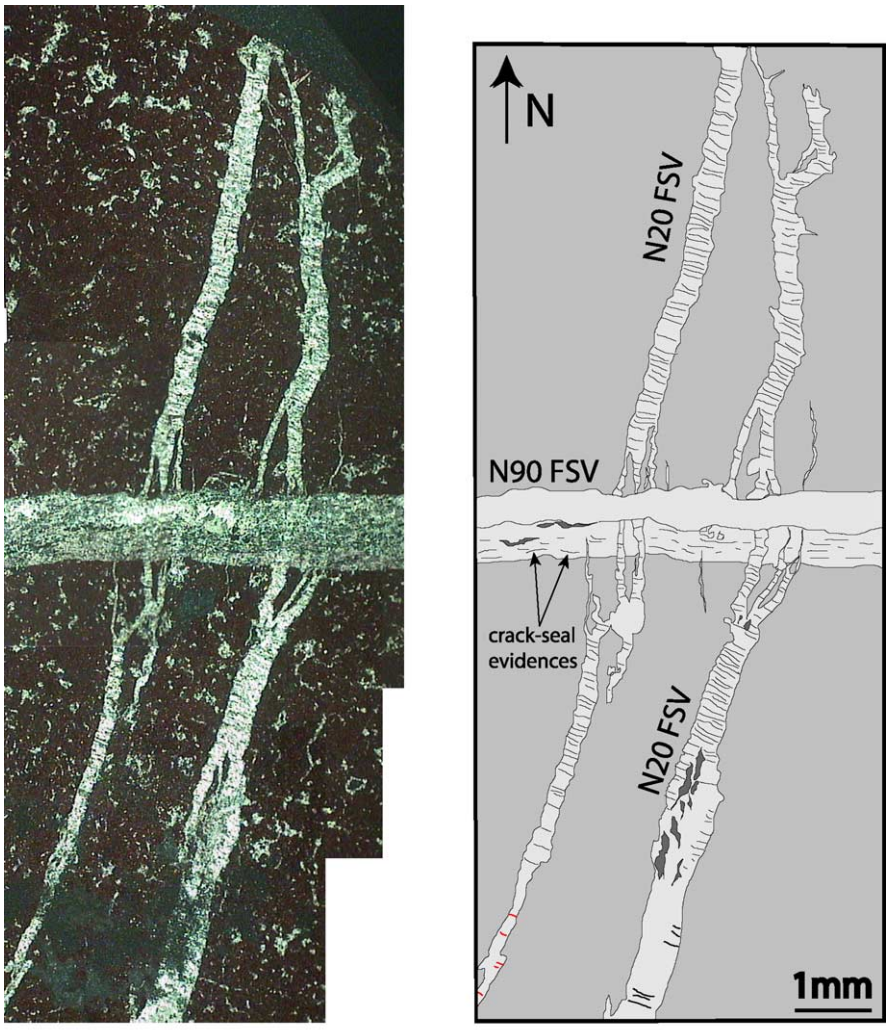

Fig. 15. (a) Photograph of a thin section showing two N20 Fibrous Slim Veins getting thinner at contact with a N90 Fibrous Slim Vein, and several stage of opening of both the N20 Fibrous Slim Veins and the N90 Fibrous Slim Vein. (b) Drawing corresponding to the photograph.

of the host rock. The Sparitic Sinuous Veins propagated in incompletely compacted sediments, and their formation was probably assisted by fluid pressure. Injecting pressurized fluids to a non-cohesive sediment may lead to complex fracturing because the response of the medium is not strictly elastic. When the N90 Fibrous Slim Veins propagated, the material had already been submitted to the compaction, and was more cohesive. The formation of the N90 Fibrous Slim

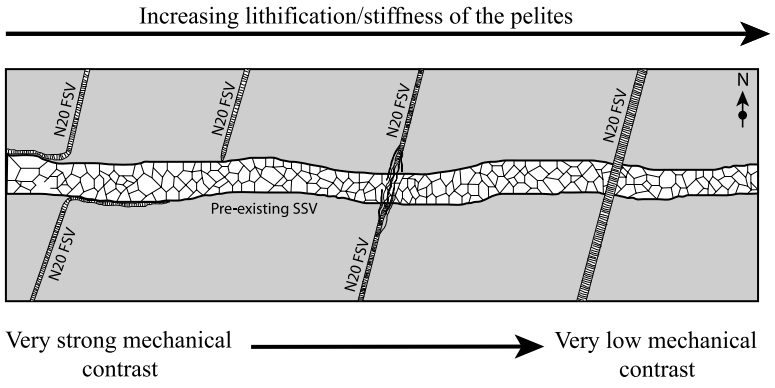

Fig. 16. Proposed model for the different mechanical behaviours of N20 propagating cracks at contact with a pre-existing Sparitic Sinuous Vein.

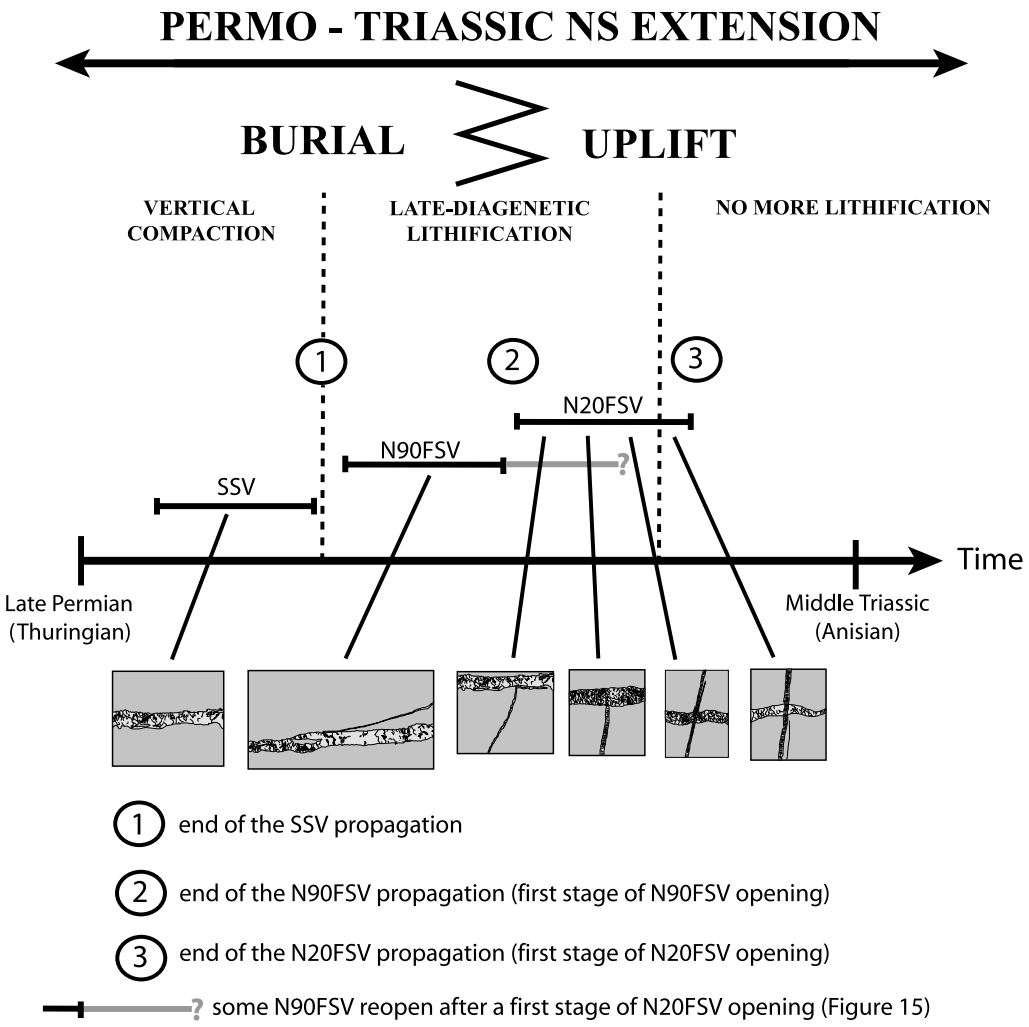

Fig. 17. Possible scenario for the formation of the three studied vein sets during the evolution of the Lodève basin.

Veins was associated with pressurized fluids (evidences of crack-seal), as it was the case for the Sparitic Sinuous Veins, but the fracturing style of the Fibrous Slim Veins is different because the mechanical behaviour of the pelites was closer to that of an elastic material at this stage.

8. Conclusions

The three main vein sets occurring in the Lodève Permian basin (Sparitic Sinuous Veins, N90 Fibrous Slim Veins and N20 Fibrous Slim Veins) show various types of intersections with complex structuring that often imply several stages of opening. The description of such intersections enabled a relative chronology between the vein sets to be realized: the N20 Fibrous Slim Veins post-date the N90 Fibrous Slim Veins, which post-date the Sparitic Sinuous Veins. Furthermore, it is shown that successive propagating cracks of one set could in certain cases crosscut the pre-existing veins of an earlier set, or could be stopped at contact with earlier veins in other cases. This implies a physical change in the interface between the pre-existing veins and the host rock during the formation of the latest cracks, attributed to an increasing lithification of the pelites.

All the observations imply that the three vein sets formed during a late stage of the basin history: the Sparitic Sinuous Veins were vertically compacted, and the Fibrous Slim Veins formed in an incompletely lithified host rock. We propose that the Sparitic Sinuous Veins formed as a result of both the NS Permo-Triassic extensional regime and fluid pressure, during the burial of the basin. The Fibrous Slim Veins formed at the beginning of the uplift of the basin, during the same NS extension (reversals between S_H and S_h accounting for the formation of the N20 Fibrous Slim Veins during the uplift of the basin). Excess in-fluid pressure may have assisted the formation of the N90 Fibrous Slim Veins.

Finally, the observed evolution in the propagation path between the Sparitic Sinuous Veins and the N90 Fibrous Slim Veins, which cannot be predicted by the stress ratio

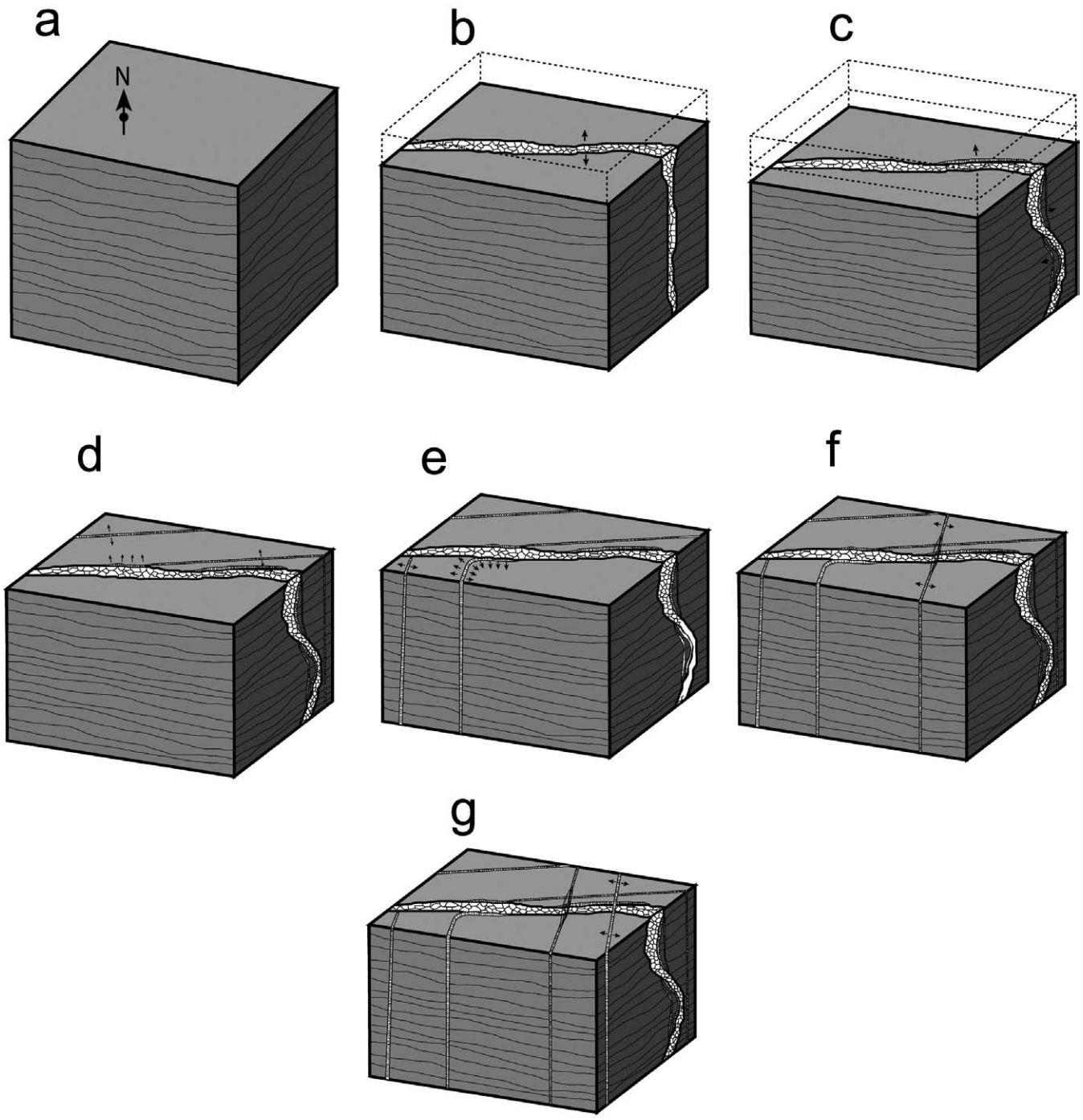

Fig. 18. Reconstitution of the different stages of formation of the three studied vein sets of the Lodève basin.

theory, is attributed to the fact that the rheology of the host rock evolved during the formation of the vein sets.

Acknowledgements

The authors thank Pascal Cortes for fruitful discussions and a critical review, which greatly improved the paper. Many thanks to Dov Bahat and Mark Evans whose comments helped to clarify the paper.

References

Auzias, V., Rives, T., Petit, J.P., 1993. Signification des côtes (rib marks) dans la cinétique de propagation des diaclases: modèle analogique dans le polyméthacrylate de méthyle (PMMA). Comptes Rendus de l'Académie des Sciences de Paris série II 317, 705–712.

Bahat, D., 1987. Jointing and fracture interactions in Middle Eocene chalks near Beer Sheva, Israël. Tectonophysics 136, 299–321.

Bahat, D., 1989. Fracture stresses at shallow depths during burial. Tectonophysics 169, 59–65.

Bahat, D., 1991. Tectono-fractography. Springer-Verlag, Berlin.

Balmelle, J.L., 1989. Géométrie et évolution du bassin permien de Lodève: subsidence autuno-saxonienne et semi-graben thuringien. MSc Thesis, Université Montpellier II.

Bazalgette, L., 2000. Lien entre la géométrie et la cinétique de propagation des fractures de mode I: étude de terrain et modélisation expérimentale. MSc Thesis, Université Montpellier II.

Becq-Giraudon, J.F., Van Den Driessche, J., 1993. Continuité de la sedimentation entre le Stéphanien et l'Autunien dans le basin de Graissessac-Lodève (sud du Massif Central): implications tectoniques. Comptes Rendus de l'Académie des Sciences de Paris série II 317, 939–945.

Bellon, H., Ellenbeger, F., Maury, R., 1974. Sur le rajeunissement de l'illite des pélites saxoniennes du Bassin de Lodève. Comptes Rendus de l'Académie des Sciences de Paris série II 278, 413–415.

Brothers, R.J., Kemp, A.E.S., Maltman, A.J., 1996. Mechanical development of vein structures due to the passage of earthquakes waves through poorly-consolidated sediments. Tectonophysics 260, 227–244.

Bruel, T., 1997. Caractérisation des circulations de fluides dans un réseau fracturé et rôle des contraintes in situ. PhD Thesis, Université Montpellier II.

Bruel, T., Petit, J.P., Massonnat, G., Guerin, R., Nolf, J.L., 1999. Relation entre écoulements et fractures ouvertes dans un système aquifère compartimenté par des failles et mise en évidence d'une double porosité de fractures. Bulletin de la Société Géologique de France 170, 401–412.

Capus, G., 1979. Matières organiques et minéralisations uranifères: exemples des bassins Permo-Carbonifères de l'Aumance (Allier) et de Lodève (Hérault). PhD thesis, Institut National Polytechnique de Lorraine.

Clément, J.Y., 1986. Minéralogie, pétrologie et géochimie du Permien de Lodéve (Hérault, France). Diagénèse précoce, altération feldspathisante et mise en place des minéralisations uranifères. PhD thesis, Ecole des Mines de Paris.

Cooke, M.L., Underwood, C.A., 2001. Fracture termination and step-over at bedding interfaces due to frictional slip and interface opening. Journal of Structural Geology 23, 223–238.

Cox, S.F., 1987. Antitaxial crack-seal vein microstructures and their relationship to displacement paths. Journal of Structural Geology 9, 779–787.

Durney, D.W., Ramsay, J.G., 1973. Incremental strains measured by syntectonic crystal growth, in: De Jong, K.A., Scholten, R. (Eds.), Gravity and Tectonics. John Wiley, New York, pp. 67–96.

Echtler, H., Malavieille, J., 1990. Extensional tectonics, basement uplift and Stephano–Permian collapse basin in a late Variscan metamorphic core complex (Montagne Noire, Southern Massif Central). Tectonophysics 177, 125–138.

Engelder, T., 1985. Loading paths to joint propagation during a tectonic cycle: an example from the Appalachian Plateau, USA. Journal of Structural Geology 7, 459–476.

Engelder, T., 1987. Joints and shear fractures in rocks, in: Atkinson, B.K. (Ed.), Fracture Mechanics of Rock. Academic Press, pp. 27–69.

Gauthier, B., Angelier, J., 1986. Distribution et signification géodynamique des systèmes de joints en contexte distensif: un exemple dans le rift de Suez. Comptes Rendus de l'Académie des Sciences de Paris série II 12, 1147–1152.

Hancock, P.L., 1985. Brittle microtectonics: principles and practice. Journal of Structural Geology 7, 437–457.

Hancock, P.L., Atiya, M.S., 1975. The development of en-echelon vein segments by the pressure solution of formerly continuous veins. Proceedings of the Geologists' Association 86-3, 281–286.

Helgeson, D.E., Aydin, A., 1991. Characteristics of joint propagation across layer interfaces in sedimentary rocks. Journal of Structural Geology 13, 897–911.

Horrenberger, J.C., Ruhland, M., 1981. Déformation progressive des sédiments permiens du bassin de Lodève (Hérault). Evolution géométrique et cinématique d'un modèle en extension par glissement-basculement. Bulletin de la Société Géologique de France 34, 75–88.

Jalabert, X., 1998. Caractérisation structurale et géochimique à l'aide du rapport isotopique ($^{87}Sr/^{86}Sr$) des colmatages carbonatés des fentes de tension dans la série Saxono-Thuringienne du bassin Permien de Lodève. MSc Thesis, Université Montpellier II.

Jones, A.P., Omoto, K., 2000. Towards establishing criteria for identifying trigger mechanisms for soft-sediment deformation: a case study of Late Pleistocene lacustrine sands and clays, Onikobe and Nakayamadaira Basins, northeastern Japan. Sedimentology 47, 1211–1226.

de Joussineau, G., Bazalgette, L., 1998. Géométrie et mécanismes de la fracturation dans le Saxonien du bassin de Lodève. Report, Université Montpellier II.

Kawakami, G., Kawamura, M., 2002. Sediment flow and deformation (SFD) layers: evidence for intrastratal flow in laminated muddy sediments of the Triassic Osawa Formation, northeast Japan. Journal of Sedimentary Research 72, 171–181.

Kimura, G., Koga, K., Fujioka, K., 1989. Deformed soft sediments at the junction between the Mariana and Yap trenches. Journal of Structural Geology 11, 463–472.

Lancelot, J., Vella, V., 1989. Datation U–Pb liasique de la pechblende de Rabejac. Mise en évidence d'une préconcentration uranifère permienne dans le bassin de Lodève (Hérault). Bulletin de la Société Géologique de France 8, 309–315.

Lancelot, J.R., de Saint André, B., de la Boisse, H., 1984. Systématique U–Pb et évolution du gisement d'uranium de Lodève (France). Mineralium Deposita 19, 44–53.

Laubach, S.E., 1988. Subsurface fractures and their relationship to stress history in East Texas basin sandstone. Tectonophysics 156, 37–49.

Laubach, S.E., Marett, R.A., Olson, J.E., Scott, A.R., 1998. Characteristics and origins of coal cleat: a review. Coal Geology 35, 175–207.

Laversanne, J., 1976. Sédimentation et minéralisation du Permien de Lodève (Hérault). PhD thesis, Université de Paris Sud, Centre d'Orsay.

Lévêque, M.H., Lancelot, J.R., Georges, E., 1988. The Betholène uranium deposit. Mineralogical characteristics and U–Pb dating of the primary U mineralization and its subsequent remobilization: consequences upon the evolution of the U deposits of the Massif Central, France. Chemical Geology 69, 147–163.

Lopez, M., 1987. Approche sédimentologique et microtectonique du Permo-Trias du bassin de Lodève. MSc Thesis, Université Montpellier II.

Lopez, M., 1992. Dynamique du passage d'un appareil térrigène à une plate-forme carbonatée en domaine semi-aride: le Trias de Lodève, Sud de la France. PhD thesis, Université Montpellier II.

Magara, K., 1975. Importance of aquathermal pressuring effect in Gulf Coast. American Association of Petroleum Geologist Bulletin 59, 2037–2045.

Magara, K., 1976. Water expulsion from clastic sediments during compaction—directions and volumes. American Association of Petroleum Geologist Bulletin 60, 543–553.

Magara, K., 1981. Mechanisms of natural fracturing in a sedimentary basin. American Association of Petroleum Geologist Bulletin 65, 123–132.

Maltman, A.J., 1988. The importance of shear zones in naturally deformed wet sediments. Tectonophysics 145, 163–175.

Maury, R., Mervoyer, B., 1973. Métamorphisme thermique des pélites permiennes du bassin de Lodève au contact d'intrusions basaltiques de tailles variées: quelques aspects minéralogiques. Bulletin de la Société Géologique de France 7, 313–320.

Nogueira, A.C.R., Riccomini, C., Sial, A.N., Moura, C.A.V., Fairchild, T.R., 2003. Soft-sediment deformation at the base of the Neoproterozoic Puga cap carbonate (southwestern Amazon craton, Brazil): confirmation of rapid icehouse to greenhouse transition in snowball earth. Geology 31, 613–616.

Odin, B., 1986. Les formations permiennes, Authunien supérieur à

Thuringien, du "bassin" de Lodève (Hérault, France): stratigraphie, minéralogie, paléoenvironnements corrélations. PhD thesis, Université d'Aix-Marseille III.

Odin, B., Doubinger, J., Conrad, G., 1986. Attribution des formations détritiques, rouges, du Permien du Sud de la France au Thuringien, d'après l'étude du bassin de Lodève: implications géologiques, paléontologiques et paléoclimatiques. Comptes Rendus de l'Académie des Sciences de Paris série II 302, 1015–1020.

Olson, J., Pollard, D.D., 1989. Inferring paleostresses from natural fracture patterns: a new method. Geology 17, 345–348.

Petit, J.P., Laville, E., 1987. Morphology and microstructures of hydroplastic slickensides in sandstone, in: Jons, M.E., Preston, R.M.F. (Eds.), Deformation of Sediments and Sedimentary Rocks Geological Society Special Publication, 29, pp. 107–121.

Petit, J.P., Massonnat, G., Pueo, F., Rawnsley, K., 1994. Rapport de forme des fractures de mode I dans les roches stratifiées: une étude de cas dans le bassin permien de Lodève (France). Bulletin du Centre de Recherches Exploration-Production Elf-Aquitaine 18, 211–229.

Pollard, D.D., Aydin, A., 1988. Progress in understanding jointing over the past century. Geological Society of America Bulletin 100, 1181–1204.

Pueo, F., 1993. Approche quantitative du rapport de forme des fractures: étude bibliographique, données de terrain. MSc Thesis, Université Montpellier II.

Ramsay, J.G., 1980. The crack-seal mechanism of rock deformation. Nature 284, 135–139.

Ramsay, J.G., Huber, M.I., 1983. The Techniques of Modern Structural Geology (Volume 1: session 13; Volume 2: sessions 25 and 27). Academic Press, London.

Renshaw, C.E., Pollard, D.D., 1994. Are large differential stresses required for straight fracture propagation paths? Journal of Structural Geology 16, 817–822.

Rives, T., 1988. L'interprétation des diaclases: approche expérimentale et application à quelques cas naturels. MSc Thesis, Université Montpellier II.

Rives, T., 1992. Mécanismes de formation des diaclases dans les roches sédimentaires: approche expérimentale et comparaison avec quelques exemples naturels. PhD Thesis, Université Montpellier II.

Rives, T., Rawnsley, K.D., Petit, J.P., 1994. Analogue simulation of natural orthogonal joint set formation in brittle varnish. Journal of Structural Geology 16, 419–429.

Rolando, J.P., Doubinger, J., Bourges, P., Legrand, X., 1988. Identification de l'Autunien supérieur, du Saxonien et du Thuringien inférieur dans le bassin de Saint Affrique (Aveyron, France). Corrélations séquentielles et chronostratigraphiques avec les bassins de Lodève (Hérault) et de Rodez (Aveyron). Comptes Rendus de l'Académie des Sciences de Paris série II 307, 1459–1464.

Saint Martin, M., 1992. Génèse et évolution structurale du bassin permien de Lodève (Hérault-France). Cuadernos de Geologia Ibérica 16, 75–90.

Saint Martin, M., Valbert, M., Robert, J.P., 1990. Contribution à la determination de l'évolution structurale des sédiments du basin permien de Lodève (Hérault, France) par l'étude microtectonique de carottes de sondages. Comptes Rendus de l'Académie des Sciences de Paris série II 311, 705–712.

Salti, C., 1995. Etude de la microfracturation et des colmatages dans le bassin permien de Lodève (Hérault, France). MSc Thesis, Université Montpellier II.

Santouil, G., 1980. Tectonique et microtectonique comparées de la distension permienne et de l'évolution post-triasique dans les bassins de Lodève, Sainte Affrique et Rodez (France, SE). PhD thesis, Université Montpellier II.

Schwehr, K., Tauxe, L., 2003. Characterization of soft-sediment deformation: detection of crytoslumps using magnetic methods. Geology 31, 203–206.

Simon, J.L., Seron, F.J., Casas, A.M., 1988. Stress deflection and fracture development in a multidirectional extension regime. Mathematical and experimental approach with field examples. Annales Tectonicae 1, 21–32.

Urai, J.L., Williams, P.F., Van Roermund, H.L.M., 1991. Kinematics of crystal growth in syntectonic fibrous veins. Journal of Structural Geology 13, 823–836.

Van Den Driessche, J., Brun, J.P., 1992. Extension post-épaississement et riftogénèse permienne en Europe. 14ème Réunion des Sciences de la Terre, 13–15 avril 1992, Toulouse.

Van Loon, A.J., 2002. Soft-sediment deformations in the Kleszczow graben (central Poland). Sedimentary Geology 147, 57–70.